Space-time evolution of monogenetic volcanism in the mafic Garrotxa Volcanic Field (NE Iberian Peninsula)
Bulletin of Volcanology, 2013, Volume 75, Number 11, Page 1
C. Cimarelli, F. Traglia, D. Rita, D. Gimeno Torrente, J-. L. Fernandez Turiel

# Space–Time evolution of monogenetic volcanism in the mafic Garrotxa Volcanic Field (NE Iberian Peninsula).

C. Cimarelli[1*], F. Di Traglia[2,3], D. de Rita[4], D. Gimeno Torrente[5], J-.L. Fernandez Turiel[6]

*corresponding author

1. Department of Earth and Environmental Sciences, Ludwig Maximilians Universitaet Muenchen, Theresienstraße 41, 80333 Munich, Germany. E-mail cimarelli@min.uni-muenchen.de; fax +49 (0) 89 2180 - 4176

2. Department of Earth Sciences, Università di Pisa, Via Santa Maria 53, Pisa, Italy, ditraglia@dst.unipi.it

3. Department of Earth Sciences, University of Firenze, Via La Pira 4, Firenze, Italy, federico.ditraglia@unifi.it

4. Dipartimento di Scienze Geologiche, Università Roma Tre, L.go Murialdo 1, Roma, Italy. E-mail derita@uniroma3.it ;

5. Department Geoquímica, Petrologia i Prospecció Geològica, Universitat de Barcelona. Carrer Martí i Franquès s/n, 08028, Barcelona, Spain. E-mail domingo.gimeno@ub.edu ;

6. Institute of Earth Sciences “Jaume Almera”, CSIC, Solè i Sabaris s/n, 08028, Barcelona, Spain. E-mail jlfernandez@ictja.csic.es

**Abstract**

We reconstructed the evolution of the volcanic activity within the central Garrotxa monogenetic Volcanic Field, the youngest volcanic area of the Iberian Peninsula, by investigating the stratigraphy of the volcanic successions and the morphologies of the monogenetic eruptive centres. The study of the volcanic succession has been conducted following the Unconformity Bounded Stratigraphic Units criteria applied to volcanic terrains. The detailed stratigraphy of the volcanic successions shows that the central GVF evolved through four main periods of volcanic activity (Synthems) represented by the eruptive products of the mafic monogenetic volcanoes and associated syn-eruptive reworked deposits (Eruptive Units) and by the inter-eruptive deposits (Epiclastic Units). The distribution and the morphology of the monogenetic eruptive centres suggest that feeder dykes emplaced according to the present stress tensor and along pre-existing fractures of the basement. The facies analysis of the deposits and their distribution shows that migration of volcanism toward the center of the basin was accompained by a trend of increasing explosivity. Episodic hydromagmatism in the central Garrotxa occurred without a specific geographic nor temporal correlation. Finally, integrating field data with the stratigraphy of water wells, we determined the volume of the volcanic deposits. The small average volume of products emitted during each eruptive period and the long quiescence separating them allows classifying the GVF as a low output rate volcanic field.

Keywords: Garrotxa; mafic volcanic field; scoria cone; monogenetic; UBSU

## Introduction

Volcanic fields in continental settings commonly consist of scattered or closely-spaced small volcanoes, mostly mafic in composition. These volcanoes are often referred to as monogenetic in that it is believed that they erupt only once and their activity rapidly wanes (Walker, 1993; Connor and Conway, 2000; Valentine and Gregg, 2008). They commonly form extensive cinder-cone fields, sometimes associated with polygenetic shield volcanoes (Tibaldi, 1995; Corazzato and Tibaldi, 2006; Dóniz et al., 2008).

The eruptive style of monogenetic basaltic volcanoes can change from Strombolian to Hawaiian to violent Strombolian in response to changing behaviour of the exsolving volatile species, magma rise-speed and the coupling between gas and melt plus crystals (Head and Wilson, 1989; Parfitt, 2004; Valentine and Gregg, 2008; Cimarelli et al., 2010).

Monogenetic volcanism has been related to high regional differential stress, in areas with variable (high or low) magma input/output rate (Takada, 1994). Low-output rate volcanic fields usually consist in a small number of widely spaced volcanoes (Valentine and Hirano, 2010), while high-output rate volcanic fields comprise densely-concentrated cones, shields and surrounding lava plains (Condit and Connor, 1996). The distribution of monogenetic volcanoes within basaltic volcanic fields is generally related to the geometry of the underlying magma source zone (Condit and Connor, 1996; Valentine and Keating, 2007; Kiyosugi et al., 2010) and/or to the presence of tectonic structures in the shallow crust (Valentine and Perry, 2007; Keating et al., 2008).

The Garrotxa Volcanic Field (GVF), the most recent volcanic area in the Iberian Peninsula (0.5-0.01 Ma, Araña et al., 1983; Puiguriguer et al., 2012), consists of more than 40 well preserved monogenetic centres, grouped in two different zones: 1) a central zone, where the younger cones are located (the central GVF), and 2) a peripheral zone, that consists of about 12 widely scattered vents (Araña et al., 1983). Despite their fairly conical morphology, some of these edifices show to have experienced a complex evolution with the alternation of predominantly magmatic activity with minor phreatic and phreatomagmatic episodes (Di Traglia et al., 2009; Gisbert Pinto et al., 2009; Martí et al., 2011). The existing datings on lavas and one paleosol from the central GVF show that the volcanic activity in this sector occurred between 247±17 ka to 11.5±1.1 ky BP (Guérin et al., 1985; Puiguriguer et al., 2012). Unfortunately the dated lavas have not been framed into a detailed stratigraphic scheme thus preventing a thorough reconstruction of the spatial-temporal variation of volcanic activity within the central GVF.

We investigated the relationship between eruptive styles and volcanoes distribution through time within the central Garrotxa tectonic depression.

The detailed stratigraphic analysis and geological mapping of the area (scale 1:5000) allowed defining the volcanic successions and their relative chronology. The facies analysis of the deposits helped us constraining the eruptive styles experienced by each volcanic centre. Volcano morphologies and their internal structures have also been examined by integrating field data and a digital elevation model (DEM) to understand the relation between volcanism and local/regional tectonics. Finally, complementing field data with water wells stratigraphy, we were able to reconstruct the top surface of the pre-volcanic basement and to define the thickness and the total volume of the volcanic deposits. Combining the existing geochronological datings and the volume estimate we have been able to determine the total output rate of the volcanism in the central GVF.

## Geological setting

*Geodynamic significance of the North East Volcanic Province of Spain*

The GVF is located about 90 km NNE of Barcelona and about 30 km NW of the city of Girona, in the pre-Pyrenees area (Fig. 1a). GFV together with the Ampurdà (AVF), Tordera (TVF) and Selva (SVF, also called southern Garrotxa; Martí et al., 2011) volcanic fields is part of the North East Volcanic Province of the Iberian Peninsula (NEVP; Araña et al., 1983) also referred as the Catalan Volcanic Zone (Martí et al., 2011).

The Neogene to Quaternary NEVP volcanism is interpreted as the result of the Pyrenees post collisional back–arc extension driven by the African slab retreat, which favoured the rise of magmas through the Iberian continental crust (Gallart et al., 1991; Zeyen et al., 1991; Martí et al., 1992). The NEVP volcanism is associated with a system of NE-SW and NW-SE regional faults that control the geometry of the main tectonic depressions in this area (Araña et al, 1983). Volcanic activity in the NEVP took place between 10 and 0.01 Ma, with the oldest eruption in the AVF and the youngest in the GVF (Donville, 1976; Araña et al., 1983). Migration of volcanism is coherent with the differential opening velocities of the western Mediterranean (Ligure – Provençal basin) during the Oligocene-Miocene, with its northern sector (Gulf of Lyons) experiencing a faster opening respect to the southern-most part (Valencia margin; Mauffret et al., 1995; Goula et al., 1999). In the same way, volcanism migrated from NE to SW. During the Pliocene - Lower Pleistocene, volcanism migrated to the NW toward the GVF in accordance with the change in the regional stress orientation from pure extensional (vertical σ1 and NW-SE σ3) to mainly strike-slip motions (vertical σ2 and NNW-SSE σ1; Goula et al., 1999). Westward migration of the extensional regime at a rate of 5 mm/yr (Vergès and Sàbat, 1999) and the consequent migration of volcanism is interpreted in terms of mechanical removal of the mantle lithosphere by buoyancy due to the migration of a thermally heterogeneous mantle (Cebrià et al., 2000). Such buoyancy would have caused the regional scale doming of the crust centred on the tectonically and volcanically active region of the Garrotxa (Lewis et al., 2000).

NEVP parental magmas are petrologically similar to those feeding the Cenozoic to Quaternary intraplate volcanism of central Europe (Massif Central, Provence Volcanic Field and Eifel Volcanic Field; Mertes and Schminke, 1985; Wilson et al., 1995; Bianchini et al., 2007; Carracedo Sánchez et al., 2012). Volcanic rocks from GVF are represented by leucite basanites, nepheline basanites and alkali olivine basalts.

*The pre-volcanic basement*

The pre-volcanic basement in the central GVF consists of Paleozoic, Eocene and Quaternary rocks. Paleozoic units underlying the Eocene successions crop out south of the studied area and are mainly constituted by plutonic and metamorphic rocks (Fig. 1b). The Eocene succession in the Garrotxa area is composed by a deepening-shallowing set of nine depositional sequences broadly represented by alluvial systems capped by delta and shallow carbonate platform systems and finally evolving into a shallowing-upward succession characterized by evaporitic deposits followed by delta and alluvial systems (Giménez-Montsant et al., 1999). These rocks have been extensively deformed and in the studied area they form E-W oriented folds dissected by normal faults roughly parallel to their axes (Gallart et al., 1991; Gimenez-Montsant et al., 1999). The Quaternary sedimentary rocks consist of fluvial and lacustrine sediments and limited travertine deposits precedent and contemporaneous to the deposition of the volcanic products (SGC, 2002, 2003).

Two major NW-striking faults, the Amer fault to the west and the Llorà fault to the east, limit the central Garrotxa tectonic depression. The tectonic depression is further limited to the north and to the south by the Valfogona thrust and the sedimentary ridge of the Serra Transversal, respectively (Fig. 1b). The GVF is mainly localized in two different sectors of the tectonic depression: the Olot-Fluvià river valley to the north and the Santa Pau-Ser river valley to the south. Some of the major faults controlling the structural architecture of the area proved to be tectonically active in historical times, generating destructive earthquakes during the Middle Ages (Fleta et al., 2001).

**The Unconformity Bounded Stratigraphic Units criteria**

The fieldwork has been conducted following the Unconformity Bounded Stratigraphic Units criteria (UBSU; Salvador, 1987, 1994), based on the hierarchy of the identified stratigraphic unconformities. The reference unit of the UBSU is the Synthem, defined as a stratigraphic body delimited by significant and demonstrable unconformities, preferably having a regional or inter–regional extension (Salvador, 1987). Given the volcanic nature of the studied successions, we adopted the UBSU methodology modified for volcanic terrains (de Rita et al., 1997; Di Traglia et al., 2013). Within the framework of the UBSU, the Eruptive Unit (as defined by Fisher and Schmincke, 1984) represents the basic lithostratigraphic unit within the Synthem (Fig. 2 for a general example). Different types of unconformities have been identified and classified according to their ranking (Fig. 3). Major unconformities (S1) extend over the whole studied area and are characterised by diffused areal erosion and are marked locally by decimetre-thick paleosols. The S1 unconformities constitute the boundary of the different Synthems. Lower rank unconformities S2, locally corresponding to paleo-gullies, limit the Eruptive and Epiclastic Units within each Synthem. Other smaller-scale unconformities (S3) are recognised within the Eruptive Units and separate primary (lavas and pyroclastic deposits) and/or syn-eruptive reworked deposits (see Fig. 3 and 4).

The study of about fifty stratigraphic sections (the more representative of which are sketched in Fig. 4) allowed making a geological map of the area (Fig. 5). Classification of the deposits has been based on their lithological characteristics, average componentry of clasts and matrix, organization and geometry and presence of sedimentary structures (Table 1), allowing the distinction between primary and volcaniclastic deposits (Table 2).

## Stratigraphy of the Central GVF

Volcanism in the Central GVF developed with the emplacement of numerous small monogenetic eruptive centres aligned with the main structural features controlling the evolution of the Central GVF tectonic depression. Volcanic activity was characterised by both effusive and explosive events that led to the emplacement of lava flows, lava sheets and the edification of spatter cones and cinder cones.

Volcanic successions have been organized in four Synthems (Valls dels Arcs Synthem, Santa Pau Synthem, Mascou Synthem, Les Tries Synthem; Fig. 5, Table 1). In each Synthem one Eruptive Unit (comprising both primary and syn-eruptive reworked deposits, Figs. 4 and 6) and one continental sedimentary unit (epiclastic inter-eruptive deposits) have been recognized. The three Epiclastic Units represent quiescence periods of the volcanic activity. The organization of the studied successions in Synthems, according to the presence of unconformities of comparable hierarchy, indicates that the volcanism in the central GVF evolved through four main periods during which several eruptions (clusters) occurred, separated by comparable unconformities (i.e. comparable pauses in the volcanic activity).

*Facies analysis and eruptive style of volcanic centres*

Facies analysis of the volcanic deposits allowed identifying the eruptive styles of the volcanoes, and the transport and sedimentation mechanisms of primary and reworked pyroclastic material. The detailed description of the deposits is resumed in Table 1. From the facies analysis of the volcanic successions belonging to each eruptive unit it is possible to reconstruct the eruptive style of each volcanic centre in the central GVF. In general volcanic activity changed from mainly effusive to prevalently explosive through time. In fact older eruptive units (Batet de La Serra EU and Puig de Mar EU, Fig. 6), were mainy characterized by the effusion of large lava sheets and lava flows through eruptive fissures. The explosive activity recorded in these early eruptions was represented by localized episodes of Hawaiian-type lava fountaining that constructed spatter ramparts and rootless lava flows. During the intermediate and final eruptive stages instead (Roca Negra EU and Croscat EU, Fig. 6), in addition to spatter ramparts and lava flows, prolonged Hawaiian and Strombolian activity led to the edification of major, younger, cinder cones. The explosive activity of the youngest Croscat EU culminated with the violent Strombolian activity of the Croscat Volcano that constitutes the highest explosivity episode of the central GVF.

## Cone morphology and morphotectonic features

### *Methodological approach*

Cone morphology and morpho-tectonic features have been analysed through a dedicated GIS based on a 5 m resolution DEM. The DEM derived from the topographic maps of the Institut Cartografic de Catalunya (scale 1:5000; contour interval 5 m).

The distribution of major morpho-structural features has been deduced combining the analysis of DEM-derived thematic maps such as slope, break in slope and slope aspect (horizontal direction to which the slope faces) with the drainage network map, following the methodology described in Cimarelli and de Rita (2006). In order to deduce the main morpho-structural trends of the pre-volcanic basement rocks, this analysis was performed on an area exceeding the extension of the volcanic deposits. The frequency of the measured lineament azimuth was plotted on rose diagrams (Fig. 7).

Information on the direction of magma-feeding fractures has been obtained for 15 eruptive centres through morphometric investigations (Table 3), following the methodology proposed by Corazzato and Tibaldi (2006). The main morphological parameters used in this analysis are the alignment of the coeval eruptive centres, elongation of the cones, alignment of depressed sectors at the crater rim and the azimuth of the breached sectors of the cones. Alignment of coeval cones, cone elongation and alignment of crater-rim depressed points are used as indicators of the direction of the feeding-fracture in the substrate, while cone breaching can either coincide with the weakest zone of the edifice or with the direction of maximum stress applied to its flanks by magma bulging or fracture propagation (Corazzato and Tibaldi, 2006; Bonali et al., 2011). Alignment of volcanic centres has been carried out through Fry spatial distribution analysis;. This method has been used to determine strain form the distribution of objects in a rock (Fry, 1979) and preferred orientation of volcanic cone alignments (Gutierrez et al., 2005).

*Morphological analysis*

Our statistical analysis of morphological lineaments in the pre-volcanic basement reveals three main populations of NW-, N- and NE-striking features (Fig. 7a). The most representative NW-striking features are oriented according to the direction of the main transtensional faults limiting the tectonic depression (Amer and Llorát faults). The analysis of the hydrographic features shows that streamlines ≥700 m are scattered in all directions with main populations represented by E-, NW-, N- and NE-oriented elements (Fig. 7b, 7b1). Respect to the morpho-structural lineaments of the substrate, the additional E-trending population accounts for the elements incising the volcanic deposits. Here volcanic deposits masked the underlying morphology of the substrate and forced the drainage system to rearrange accordingly. When restricting the analysis to hydrographic features ≥800 m, the resulting rose-diagram further higlights this effect (Fig. 7b2).

Investigations on the cone spatial distribution and cone morphology provided information on the stress tensor driving the emplacements of feeder dikes and their interaction with pre-existing fractures in the basement. Both alignment of depressed sectors of crater rim and spatial distribution of eruptive centres reveal direction of NNW- to NW-striking eruptive fractures (Fig. 7c, 7d; Table 3). Alignments of coeval eruptive centres also show ENE to NE directions like in the case of the Garrinada-Montsacopa-Montolivet cones. It is worth noting that the azimuths of the breaching sectors are oriented orthogonal to the eruptive fractures determined by using the other three morphological parameters, thus suggesting that cone breaching more likely occurred by lava accumulation or bulging of the flanks (Nolesini et al., 2013).

Volumes of the ejecta constructs have been determined by combining field measurements with the DEM analysis. The volume of the cones has been calculated using the DEM surface enclosed in the cone basal area (defined using both slope map and direct field observation), while lava flow volume was calculated by multiplying the flow area by the observed mean thickness (Tab. 3). To better constrain the change in flow thickness, several longitudinal profiles were made following the methodology described by Rodriguez-Gonzalez et al. (2010).

Volumes of the ejecta constructs vary from $10^6$ to $10^8$ $m^3$ dense rock equivalent (DRE). Major scoria cones (Croscat, Monsacopa and Garrinada), characterized by larger volumes and a volcanic succession mainly constituted by lapilli and ash, are located in correspondence of the depocentre of the tectonic depression, while the smaller ones, characterized by lower volumes and coarse-grained materials, are located near the valley margins and are associated to larger volume lava flows.

The Santa Margarida volcano is the only maar-type eruptive centre in the studied area. The thin deposits of this eruptive centre drape the partially excavated Eocene basement and are found intercalated in the eruptive succession of the near Croscat Volcano (Martí et al., 2011). As already reported by Di Traglia et al. (2009), here is important to note that the geometry and the distribution of the deposits related to the Croscat EU indicate that volcanic activity occurred contemporaneously from multiple vents (Santa Margarida, Croscat, Pomareda and Puig Astrol) along a NNW–striking fracture.

**Geometry and volume of the volcanic products**

In order to estimate the volume of the volcanic material in the central GVF, we modelled the top surface of the Eocene succession based on the stratigraphy of water wells (Custodio Gimena et al., 1984) and field data. The volume of material comprised between the topographic surface and the top Eocene surface was determined using the GIS by subtracting the elevations of the two surfaces. The thickness of the major cone-building material has also been subtracted, in order to highlight the depocentres in the pre-volcanic basement. Considering the negligible thickness of the epiclastic material with respect to that of the volcanic products, we estimated the total volume of the volcanics to be about 0.5 $km^3$ DRE.

This procedure allowed to image the geometry of the sedimentary basin and to correlate the thickness variation of the deposits with the distribution of the volcanic edifices within the tectonic depression.

The map of Fig. 8a shows two depressed areas where volcanic products are thicker: one corresponds to the Olot village, while the other is located in the central sector of the tectonic depression in correspondence of the Croscat volcano. The Olot village depression, where the Garrinada and Montsacopa scoria cones are located, hosts a thickness of about 30 m of volcanic material, constituted by lavas and subordinately pyroclastic deposits. The second depression (well constrained by water-well log data) extends roughly E-W and hosts a thickness of about 160 m of volcanic products (Fig. 8b), thus identifying a basin depocentre at close distance from the Croscat-Pomareda cones. In both cases the occurrence of the maximum thickness of volcanic deposits corresponds to the location of the major volcanic edifices of the central GVF.

## Discussion

*Time evolution of the volcanic activity*

According to the stratigraphy proposed in this work, each Eruptive Unit represents a series of eruptions clustered in time, occurring between 247±17 and 11.5±1.1 ka (Fig. 4; Guérin et al. 1985; Puiguriguer et al. 2012).

Although we carefully reconstructed the relative chronology of the eruptive products, existing geochronological data do not allow a good constraint of the absolute duration of the eruptive and quiescence periods. We can infer that quiescence between the eruptive periods must have been long enough to allow the formation of the decimetre-thick paleosols and metric erosive surfaces observed in the field (Fig. 3). In particular, given the unfavourable paleoclimatic conditions for mature soil formation, established during the Quaternary in the Pyrenees region (Pallàs et al., 2006), the thickness of the paleosols and the extension of the major erosive surfaces (S1) remark quite a long interval of inactivity (of the order of tens of ka based on the available datings; Guérin et al., 1985).

Recent radiocarbon datings of the paleosol contained in the Lower Bosquet Unit (Puiguriguer et al., 2012), coupled with the age (determined by thermoluminescence on plagioclase crystals) of the Upper Santa Pau lava in the upper Roca Negra EU (28.1±2.6 ka; Guérin et al., 1985) indicate a quiescence of about 15 ka between the two last eruptive units. The same calculation can be made for the time interval between Valls dels Arcs and Santa Pau synthems. Considering the age of the Batet de La Serra Lava (247±17 ka, Guérin et al., 1985) and Garrinada Lava (132±12 ka, Guérin et al., 1985), a quiescence period of about 115 ka can be estimated. The datings available for the Lower Santa Pau Lava (Puig de Mar EU) and the Upper Santa Pau Lava (Roca Negra EU) suggest a maximum duration of the Roca Negra EU of about 82 ka.

*Spatial evolution of the volcanic activity*

The volcanic activity developed through time with a progressive vent migration from the margin toward the center of the tectonically controlled depression (Fig. 9). This migration is likely to have been favored by a progressive symmetrical extension of the basin as testified by the distribution of maximum thickness of volcanic deposits along the axis of the Olot-Santa Pau valley. Cinder cones in the central GVF are aligned along NNW to NW and ENE to NE directions while morphological characteristics of the cones (cone and crater elongation) prevalently suggest that feeder dykes followed NW to NNW directions. This is in general agreement with the orientation of morphostructural lineaments of the pre-volcanic basement. Magma ascending into the crust is likely to be captured by shallow reactivated faults and fractures, therefore dykes might have near-surface orientations that are not simply perpendicular to the least principal stress direction (Connor and Conway, 2000; Valentine and Perry, 2007; Le Corvec et al., 2013). Our data show that in the central GVF feeder dikes more likely intruded along pre-existing fractures of the substrate. It is interesting to note that the most recent Croscat EU, which also represents the peak of explosive activity, has been alimented by feeder dikes oriented NNW (Fig. 7), i.e. congruently with the orientation of the present stress tensor in the area (Goula et al., 1999).

*Eruptive style and volcanic output rate*

Migration of volcanism toward the center of the basin coincided with a trend of increasing explosivity, as testified by the facies analysis of the deposits. The occurrence of progressively higher explosive activity is characteristic of the volcanoes in the central part of the tectonic depression, where more complex and younger volcanic centres displaying violent Strombolian and phreatomagmatic activity are located. A shift in eruptive style from predominantly effusive and spattering activity in the older and marginal eruptive vents (Batet de La Serra EU and Puig de Mar EU), to more complex and intense activity in the younger and central ones (Roca Negra EU and Croscat EU), is recorded in the stratigraphic succession and facies distribution of the deposits within the eruptive units. Younger eruptions display a broader range of eruptive styles, as occurred during the Croscat eruption with the shift in eruptive intensity from Hawaiian-Strombolian to violent Strombolian (Di Traglia et al., 2009) and the occurrence of a phreatomagmatic episode at the contemporaneously active Santa Margarida volcano (Martí et al., 2011). The dynamics of this eruption, as compared to similar studied eruptions (Valentine et al., 2005; Pioli et al., 2008; Guilbaud et al., 2009), suggests the occurrence of very high flux of gas-charged magma during this stage of volcanism. Phreatomagmatism occurred in volcanoes located on both high-transmissivity (Monsacopa, Garrinada) and low-transmissivity aquifers (Santa Margarida, Martí et al., 2011), without a specific correlation with aquifer permeability.

In order to constrain the magmatic input rate in the central GVF, we combined volumetric data of emitted products with the tectonic extension rate and the available geochronological datings. We plotted central GVF data (Fig. 10) in the differential-stress versus normalized output-rate diagram proposed by Takada (1994). We used the 0.05 – 0.125 mm/yr vertical slip rate deduced by Fleta et al. (2001) for the Amer fault as an order of magnitude estimate of the differential stress in the studied area during the Quaternary. The results show that the GVF can be classified as a low output rate / small differential stress volcanic field characterized by low average volume of products emitted during each eruptive cluster and by long quiescence period separating them.

## Conclusive remarks

We investigated the geological and morphological evolution of the central area of the Garrotxa Volcanic Field and determined the relationship between eruptive styles and volcanoes distribution through time within the central Garrotxa tectonic depression.

The main outcomes of this study can be summarized as follows:

- Each recognized synthem bounded by major unconformities (S1) comprises the products of the volcanic activity and its syn-eruptive reworked deposits (Eruptive Units) and of products of erosion and re-deposition processes (Epiclastic Units). The time period separating the eruptive and syn-eruptive deposition from the widespread erosion and deposition of epiclastic material is represented by the S2 unconformity surfaces. The quiescence period between two eruptive units is represented in the GVF stratigraphic record by the unconformities produced by erosion or by the sedimentary (epiclastic) deposits, bounded at the bottom and at the top by S2 and S1 unconformities, respectively. The eruptive units represent the products of one or more eruptions clustered in time separated by time-breaks long enough to produce significant unconformities (S3 surfaces).
- Cinder cones morphologies and their alignments in the studied area suggest that feeder dykes followed the orientation of local structural lineaments, according to the active stress tensor which determines the strike-slip tectonic regime active in the NEVP since the Pliocene-Pleistocene.
- The facies analysis and distribution of the deposits shows that the migration of volcanism toward the center of the basin coincided with a trend of increasing explosivity through time. Phreatomagmatism occurred without a specific geographic correlation and independently from the permeability characteristics of the aquifer underlying the eruptive centres.
- Given the small average volume of products emitted during each eruptive cluster and the long quiescence between them (15 and 115 ka), GVF can be

classified as a low output rate /small differential stress volcanic field.

- The use of the UBSU stratigraphy in volcanic terrains confirms to be a powerful tool to unravel the spatial and temporal evolution of volcanic systems. In particular the versatility of this methodology based on the recognition of surfaces with relative hierarchy allows its application to volcanic areas with different geographic extension. The use of the UBSU results particularly useful in basaltic monogenetic volcanic fields where the homogeneous chemical composition of the deposits would disfavour the use of petro-chemical mapping criteria.
- Moreover, given the lack of widely dispersed tephra blankets (only exception being the products of the Croscat EU), the use of tephrostratigraphic correlation (i.e. Molloy et al., 2009) was here impossible. On the contrary, the correlation of widely extended unconformity surfaces and the associated syn- and inter-eruptive deposits made here possible the stratigraphic correlation between widely-spaced and low-output rate volcanic centres.

## Acknowledgments

The authors are grateful to the Parc Natural de la Zona Volcanica de la Garrotxa for logistical support. We thank G. Gisbert and M. Aulinas for photos and assistance during the fieldwork and also M.N. Gibauld and A. Tibaldi for insightful and constructive review of the manuscript. This research was carried out in the framework of the Research Group PEGEFA (SGR-2005-795; AGAUR, DURSI de la Generalitat de Catalunya) and partially funded by the the Project CGL2007-63727/BTE of the Spanish Ministry of Education and Science. F.DiT. benefited of a mobility scholarship from Università degli Studi Roma Tre.

476

## References

Araña, V., Aparicio, A., Martìn, C., Garcìa, L., Ortiz, R., Vaquer, R., Berberi, F., Ferrara, G., Albert, J., Gassiot, X., 1983. El vulcanismo neògeno – cuaternario de Cataluña: Caracteres estructurales, petrològicos y geodinàmicos. Acta Geologica Hispanica T.18,1, 1 – 17.

Bianchini, G., Beccaluva, L., Bonadiman, C., Nowell, G., Pearson, G., Siena, F., Wilson, M., 2007. Evidence of diverse depletion and metasomatic events in harzburgite-lherzolite mantle xenoliths from the Iberian plate (Olot, NE Spain): Implications for lithosphere accretionary processes. Lithos, 94, 25-45, ISSN 0024-4937, http://dx.doi.org/10.1016/j.lithos.2006.06.008.

Bonali, F., Corazzato, C., Tibaldi, A., 2011. Identifying rift zones on volcanoes: an example from La Réunion Island, Indian Ocean. Bull. Volcanol., 73, 347–366.

Carracedo Sánchez, M., Sarrionandia, F., Arostegui, J., Eguiluz, L., Gil Ibarguchi, J.I., 2012. The transition of spatter to lava-like body in lava fountain deposits: features and examples from the Cabezo Segura volcano (Calatrava, Spain), Journal of Volcanology and Geothermal Research, Volumes 227–228, 1-14.

Cassidy, J., Locke, CA. 2010. The Auckland volcanic field, New Zealand: Geophysical evidence for structural and spatio-temporal relationships. Journal of Volcanology and Geothermal Research, 195, 127-137 http://dx.doi.org/10.1016/j.jvolgeores.2010.06.016

Cebrià, J.M., López – Ruiz, J., Doblas, M., Oyarzun, R., Hetogen, J., Benito, R., 2000. Geochemestry of the Quaternary alkali basalts of Garrotxa (NE Volcanic Province, Spain): a case of double enrichment of the mantle lithosphere. Journal of Volcanology and Geothermal Research, 102, 217 – 235.

Cimarelli, C. and de Rita, D., 2006. Structural evolution of the Pleistocene Cimini trachytic volcanic complex (Central Italy). Bulletin of Volcanology, 68, 538–548.

Cimarelli, C., Di Traglia, F., Taddeucci, J., 2010. Basaltic scoria textures from a zoned conduit as precursors to violent Strombolian activity. Geology, 38; 439–442; http://dx.doi.org/10.1130/G30720.1

Condit, C.D. and Connor, C.B., 1996. Recurrence rates of volcanism in basaltic volcanic fields: An example from the Springerville Volcanic Field, Arizona. Geological Society of America Bulletin, 108, 1225–1241.

Connor, C.B. and Conway, F.M., 2000. Basaltic volcanic fields. In: H. Sigurdsson, B.F. Houghton, S.R. McNutt, H. Rymer and J. Stix, Editors, Encyclopedia of Volcanoes, Academic Press, San Diego, pp 331 – 343.

Corazzato, C., and Tibaldi, A., 2006. Fracture control on type, morphology and distribution of parasitic volcanic cones: An example from Mt. Etna, Italy. Journal of Volcanology and Geothermal Research 158, 177–194.

Custodio Gimena, E., Vifials, E., Pascual, J.M., Bayò, A. and Domenech, J., 1984. Plan Hidrològico del Pirineo Oriental: Area de Olot-Alto Fluvià. Confederaciòn Hidrográfica del Pirineo Oriental, unpubl, rep., 46 pp.

de Rita, D., Giordano, G., Milli, S., 1997. Forestepping-backstepping stacking pattern of volcaniclastic successions: Roccamonfina volcano, Italy. Journal of Volcanology and Geothermal Research, 78, 267-288, http://dx.doi.org/10.1016/S0377-0273(97)00005-X.

Di Traglia, F., Cimarelli, C., de Rita, D., Gimeno Torrente, D., 2009. Changing eruptive styles in basaltic explosive volcanism: Examples from Croscat complex scoria cone, Garrotxa Volcanic Field (NE Iberian Peninsula). Journal of Volcanology and Geothermal Research, 180, 89 – 109. http://dx.doi.org/10.1016/j.jvolgeores.2008.10.020.

Di Traglia, F., Pistolesi, M., Rosi, M., Bonadonna, C., Fusillo, R., Roverato., M., 2013. Growth and erosion: The volcanic geology and morphological evolution of La Fossa (Island of Vulcano, Southern Italy) in the last 1000 years. Geomorphology, 194, 94-107.

Dóniz, J., Romero, C., Coello, E., Guillén, C., Sánchez, N., García-Cacho, L., García, A., 2008. Morphological and statistical characterisation of recent mafic volcanism on Tenerife (Canary Islands, Spain). Journal of Volcanology and Geothermal Research, 173, 185 – 195.

Donville, B., 1976. Géologie Neogène de la Catalogne Orientale. Bull. B.R.G.M., 2ème serie, Sect. IV, 177 – 210.

Fisher, R.V. and Schmincke, H.-U., 1984. Pyroclastic Rocks. Springer – Verlag, Berlin.

Fleta, J., Santanach, P., Martínez, P., Grellet, B., Masana, E., 2001. Preliminary geologic, geomorphologic and geophysical studies for the paleoseismological analysis of the Amer fault (NE Spain). Netherlands Journal of Geosciences 80, 243-253.

Fry, N., 1979. Random point distribution and strain measurement in rocks. Tectonophysics, 60, 89-105.

Gallart, J., Pous, J., Boix, F., Hirn, A., 1991. Geophysical constraints on the crustal structure of the Olot Volcanic area, NE of the Iberian peninsula. Journal of Volcanology and Geothermal Research, 47, 33 – 44.

Gimenez-Monsant, J., Calvet, F., Tucker, M.E. , 1999. Silica diagenesis in Eocene shallow-water platform carbonates, southern Pyrenees. Sedimentology, 46, 969 – 984.

Gisbert Pinto, G., Gimeno Torrente, D., Fernandez-Turiel, J.L., 2009. Eruptive mechanisms of the Puig de La Garrinada volcano (Olot, Garrotxa Volcanic Province, Northeastern Spain): a methodological study developed on proximal pyroclastic deposits. Journal of Volcanology and Geothermal Research, 180, 259-276.

Goula, X., Olivera, C., Fleta, J., Grellet, B., Lindo, R., Rivera, L.A., Cisternas, A., Carbon, D., 1999. Present and recent stress regime in the eastern part of the Pyrenees. Tectonophysics, 308, 487-502.

Guérin, G., Behamoun, G., Mallarach, J.M., 1985. Un exemple de fusió parcial en medi continental. El vulcanisme quaternari de la Garrotxa. Vitrina, Museu Comarcal de la Garrotxa, nº 1, pp 19-26.

Guilbaud, M.N., Siebe, C., Agustín-Flores, J. 2009. Eruptive style of the young high-Mg basaltic-andesite Pelagatos scoria cone, southeast of México City. Bulletin of Volcanology, 71, 859-880. http://dx.doi.org/10.1007/s00445-009-0271-0

Gutiérrez, F., Gioncada, A., González Ferran, O., Lahsen, A., Mazzuoli, R., 2005. The Hudson Volcano and surrounding monogenetic centres (Chilean Patagonia): An example of volcanism associated with ridge–trench collision environment. Journal of Volcanology and Geothermal Research, 145, 207-233

Head, J.W. and Wilson, L., 1989. Basaltic pyroclastic eruptions: influence of gas-release patterns and volume fluxes on fountain structure, and the formation of cinder cones, spatter cones, rootless flows, lava ponds and lava flows. Journal of Volcanology and Geothermal Research, 37, 261-271.

IGC (Institut Geològic de Catalunya) 2002. Cartografia Temàtica. Sèrie Mapa Geològic de Catalunya. Santa Pau. Available at http://www1.igc.cat/web/gcontent/pdf/mapes/igc_GT1_295q11_75x23_v1g.pdf

IGC (Institut Geològic de Catalunya) 2003. Cartografia Temàtica. Sèrie Mapa Geològic de Catalunya. Olot. Available at http://www1.igc.cat/web/gcontent/pdf/mapes/igc_GT1_257q12_75x22_v1g.pdf

Keating, G.N., Valentine, G.A., Krier, D.J., Perry, F.V., 2008. Shallow plumbing systems for small-volume basaltic volcanoes. Bulletin of Volcanology, 70, 563–582, http://dx.doi.org/10.1007/s00445-007-0154-1

Kiyosugi, K., Connor, C.B., Zhao, D., Connor, L.J., Tanaka, K., 2010. Relationships between volcano distribution, crustal structure, and P-wave tomography: an example from the Abu Monogenetic Volcano Group, SW Japan. Bulletin of Volcanology 72, 331–340, http://dx.doi.org/10.1007/s00445-009-0316-4

Le Corvec, N., Spörli, K.B., Rowland, J., Lindsay, J. 2013. Spatial distribution and alignments of volcanic centers: clues to the formation of monogenetic volcanic fields. Earth-Sci. Rev. 124, 96-114. http://dx.doi.org/10.1016/j.earscirev.2013.05.005

Lewis, C., Vergés, J., Marzo., M., 2000. High mountains in a zone of extended crust: Insights into the Neogene-Quaternary topographic development of northeastern Iberia. Tectonics, 19, 86–102.

Martí, J., Mitjavila, J., Roca, E., Aparicio, A. 1992. Cenozoic magmatism of the Valencia trough (Western Mediterranean): relationship between structural evolution and volcanism. Tectonophysics, 203, 145-165.

Martí, J., Planaguma, L., Geyer, A., Canal, E., Pedrazzi, D., 2011. Complex interaction between Strombolian and phreatomagmatic eruptions in the Quaternary monogenetic volcanism of the Catalan Volcanic Zone (NE of Spain). Journal of Volcanology and Geothermal Research, 201, 1-4, 178-193, http://dx.doi.org/10.1016/j.jvolgeores.2010.12.009.

Mauffret, A., Pascal, G., Maillard, A. and Gorini, C., 1995. Tectonics and deep structure of the north-western Mediterranean Basin. Mar. Petrol. Geol., 12, 645–666.

Mertes, H. and Schmincke, H.-U., 1985. Mafic potassic lavas of the Quaternary West Eifel volcanic field. Contribution to Mineralogy and Petrology. 89, 330-345.

Molloy, C., Shane, P., Augustinus, P., 2009. Eruption recurrence rates in a basaltic volcanic field based on tephra layers in maar sediments: Implications for hazards in the Auckland volcanic field. Geological Society of America

Bulletin, 121 (11-12), 1666-1677.

Nolesini, T., Di Traglia, F., Del Ventisette, C., Moretti, S. and Casagli, N., 2013. Deformations and slope instability on Stromboli volcano: integration of GBInSAR data and analogue modeling. Geomorph., 180-181, 242–254.

Pallàs, R., Rodés, A., Braucher, R., Carcaillet, J., Ortuño, M., Bordonau, J., Bourlès, D., Vilaplana, J.M., Masana, E.and Santanach, P., 2006. Late Pleistocene and Holocene glaciation in the Pyrenees: a critical review and new evidence from $^{10}$Be exposure ages, south-central Pyrenees. Quaternary Science Review, 25, 2937-2963.

Parfitt, E., 2004. A discussion of the mechanisms of explosive basaltic eruptions. Journal of Volcanology and Geothermal Research, 134, 77 – 107.

Pioli, L., Erlund, E., Johnson, E., Cashman, K., Wallace, P., Rosi, M., and Delgado Granados, H. 2008, Explosive dynamics of violent Strombolian eruptions: The eruption of Parícutin Volcano 1943–1952 (Mexico). Earth and Planetary Science Letters, 271, 359–368.

Puiguriguer, M., Alcalde, G., Bassols, E., Burjachs, F., Expósito, I., Planagumà, L., Saña, M., Yll, E., 2012. $^{14}$C dating of the last Croscat volcano eruption (Garrotxa Region, NE Iberian Peninsula). Geologica Acta, 10, 43-47.

Rodriguez-Gonzalez, A., Fernandez-Turiel, J.L., Perez-Torrado, F.J., Gimeno, D., Aulinas, M., 2010. Geomorphological reconstruccion and morphometric modelling applied to past volcanism. Int. J. Earth Sci., 99, 645–660.

Salvador, A., 1987. Unconformity-bounded stratigraphic units. Geological Society of America  Bulletin, 98, 232-237.

Salvador, 1994. International Stratigraphic Guide. A Guide to Stratigraphic Classification, Terminology and Procedure, Edited by The International Union of Geological Sciences and The Geological Society of America.

SGC (Servei Geològic de Catalunya), 1989. Mapa Geològic de Catalunya escala 1:250.000. Generalitat de Catalunya.

Takada, A., 1994. The influence of regional stress and magmatic input on styles of monogenetic and polygenetic volcanism.  Journal of Geophysical Research, vol. 99, no. B7, 563-573.

Tibaldi, A., 1995. Morphology of pyroclastic cones and tectonics. J. Geophys. Res. 100 (B12), 24521–24535.

Valentine, GA., Krier, D., Perry, FV., Heiken, G., 2005. Scoria cone construction mechanisms, lathrop wells volcano, southern Nevada, USA. Geology, 33, 629-632 http://dx.doi.org/10.1130/G21459

Valentine, G.A., Keating, G.N., 2007. Eruptive styles and inferences about plumbing systems at Hidden Cone and Little Black Peak scoria cone volcanoes (Nevada, U.S.A.). Bulletin of Volcanology, 70, 104–113. http://dx.doi.org/10.1007/s00445- 007-0123-8.

Valentine, G. and Perry, F., 2007. Tectonically controlled, time-predictable basaltic volcanism from lithospheric mantle source. Earth Planetary Science Letters, 261, 201 – 216.

Valentine, G.A. and Gregg, T.K.P. 2008. Continental basaltic volcanoes - Processes and problems. Journal of Volcanology and Geothermal Research, 177, 857 – 873. http://dx.doi.org/10.1016/j.jvolgeores.2008.01.050

Valentine, G. and Hirano, N,, 2010. Mechanisms of low-flux intraplate volcanic fields—Basin and Range (North America) and northwest Pacific Ocean. Geology, January, 38; p. 55–58; http://dx.doi.org/10.1130/G30427.1

Vergés, J., and Sàbat, F., 1999. Constraints on the western Mediterranean kinematics evolution along a 1,000-km transect from Iberia to Africa., in Durand, B., Jolivet, L., Horvath, F., and Séranne, M., eds., The Mediterranean basins: Tertiary extension within the Alpine orogen. Geological Society Special Publication, 156, 63-80.

Walker, G.P.L., 1993. Basaltic-volcano system. In Magmatic process and plate tectonics, Geological Society, London, Special Pubblication, 76, 3-38.

Wilson, M., Downes, H., Cebrià, J.M., 1995. Contrasting fractionation trends in coexisting continental alkaline magma series; Cantal, Massif Central, France. Journal of Petrology, 36, 1729 – 1753.

Zeyen, H.J., Banda, E., Klingelé E., 1991. Interpretation of magnetic anomalies in the volcanic area of north-eastern of Spain. Tectonophysics, 192, 201 – 210.

**Figure captions**

Fig. 1. a) North-east Volcanic Province of Spain. AVF: Ampordà Volcanic Field; TVF: Tordera Volcanic Field; SVF: Selva Volcanic Field; GVF: Garrotxa Volcanic Field. Major structural lineaments on-land and off-shore are reported (after SGC, 1989 and Mauffret et al. 1995). b) Schematic geological map of the GVF. Modified after SGC (1989).

Fig 2. Synthetic explanation of the UBSU methodology. The hypothetic cross section shows the hierarchical relations between unconformity surfaces and the bounded stratigraphic units. A basal unconformity separates the pre-volcanic basement (Prv) from the volcanic deposits. Volcanic deposits are divided into four synthems separated by S1 unconformities (in red). Synthems are formed by primary volcanic deposits (lavas: L; and pyroclastic: P), their syn-eruptive volcaniclastic deposit (Vc) and by the epiclastic deposits (Ep) representing the inter-eruptive sedimentation. Primary and syn-eruptive volcanic deposits form the eruptive units (EU) and are separated by the epiclastic units (Ep) by lower hierarchy S2 unconformities (in blue).

Fig. 3. Main stratigraphic log correlation of the central area of the GVF. The correlations allowed organizing the volcanic successions into four synthems, separated by S1 unconformities of comparable hierarchy (red lines). Each Synthem is composed of one Eruptive Unit, in its turn composed of more than one eruptive episode, and of one Epiclastic Unit (limited by S2 unconformities: blue lines) representing intereruptive sedimentation.

Fig. 4. Example of stratigraphic unconformities: a) S1 unconformity between Mascou Synthem (*RN* and *LB* units) and Les Tries Synthem (*CCU, CMU* and *CBU* units). S2 unconformity lies between *RN* (pyroclatic deposits related to the Roca Negra scoria cone) and *LB* (epiclastic) units. b) S1 unconformities between Mascou Synthem (*LB* unit) and Les Tries Synthem (*CMU, CBU* and *UB* unit). S2 unconformity lies between *CBU* (syn-eruptive reworking) and *UB* (epiclastic) units. Several lower-hierarchy unconformities (S3) lie between different pyroclastic deposits (*CCU*, *CMU*, *CBU*) within the same Croscat EU.

Fig. 5. (a) Geological map of the central GVF area (descriptions and geometry of the Eocene rocks from IGC, 2002, 2003); (b) Legend of the geological map and geochronological datings available in the literature (Guérin et al., 1985). Asterisk refers to $^{14}C$ datings from Puiguriguer et al., 2012.

Fig. 6. Different type of facies in primary deposits: a) massive to well laminated, lapilli to ash scoria blanket (Violent Strombolian style, Croscat EU) topped by

columnar-jointed lava; b) welded bombs and spatter agglomerates of the Puig de Mar EU, produced during Hawaiian-style lava fountaining; c) bedded scoria deposits of the Roca Negra EU (Roca Negra scoria cone), produced during Strombolian-type eruptions; d) massive to well bedded, lapilli to ash scoria blanket (Violent Strombolian style, Croscat EU), topped with wavy-bedded scoria-rich sand (post-eruptive reworking) and massive sand with Eocene pebble lenses (inter-eruptive reworking).

Fig. 7. DEM-derived maps of morphological elements: A) morphotectonic lineaments and related rose diagram (A1); B) drainage network elements; rose diagrams of hydrological elements $\geq$700 m (B1) and $\geq$800 m (B2); C) direction of elongation (yellow) and breaching (red) of cones and craters; D) Fry plot describing the spatial distribution of the cones and their preferential alignments.

Fig. 8. a) Isopach map of the volcanic and volcanoclastic deposits overlying the sedimentary basement. Two major depocentres are visible along the main axis of the Santa Pau-Olot valley. Open squares show the location of stratigraphic sections while crosses represent the location of water-well logs. The position of major cones is also reported (black triangles). b) Simplified geological section of the central GVF area highlighting the thickness of the volcanic deposits.

Fig. 9. Vent migration during the four Eruptive Units. The oldest vents (Batet de La Serra EU and Puig de Mar EU) are located near the structural highs, while the youngest (Roca Negra EU and Croscat EU) are located at the centre of the tectonic depression

Fig. 10. Differential-stress data versus normalized output-rate plot (following Takada, 1994). GVF can be classified as a low-output rate, tectonically controlled volcanic field, which activity is mainly controlled by the active tectonics in the NE Catalunya region (stress value from Fleta et al., 2001).

**Table captions**

Table 1. Summary of the lithofacies characteristics of the recognized eruptive units.

Table 2. Summary of the lithofacies characteristics of the reworked deposits.

Table 3. Morphometric parameters of the volcanic centres. For the Santa Margarida volcano, only the morphometric parameters of the associated scoria rampart have been extrapolated.

Dear Prof. Smith,

This letter accompanies the revision of the manuscript "Space-time evolution of monogenetic volcanism in the mafic Garrotxa Volcanic Field (NE Iberian Peninsula)".
We really would like to acknowledge the reviewers for the detailed job done on the first submitted manuscript. We welcomed many of the comments and also understand that some points raised in the reviews were caused by the unclear presentation of our data. We have hence modified the manuscript accordingly and we believe now those points are better explained.

As for the specific corrections of the text, suggestions of re-wording from the two reviewers have been accepted and modifications have been made throughout the manuscript accordingly. Also minor changes to the figures and formatting of the tables requested by the reviewers in the annotated manuscript have been made.

Below follows a detailed list of the changes done in response to the major reviewers comment.

L33 - 40
The abstract has been rephrased according to the corrections made in the text and suggestions of the reviewers.

L94 -99
Text has been added describing the existence of geochronological datings in the literature (Guérin et al., 1985) and evidencing that dating has been performed on eruptive products (mainly lavas) without taking into account the relative stratigraphy of the eruptive products. Initially we used the word "scant" referred to the gechronological datings arising the criticism of reviewer #1. We agree that the word wasn't used properly, therefore we added this extra text in the introduction.

L132 -135
Responding to point 1) of reviewer #2, here in the text referring to the opening phase of the Mediterranean Sea we added geographic references to present Mediterranean coastline in order to be easily recognized in Fig. 1a, which has been modified accordingly.

L158 – 163
Responding to point 2) of reviewer #2, here we added the description of the Eocene rocks constituting the pre-volcanic basement that was somehow gone missing in the early submitted version of the manuscript.

L179-255 and Fig 2.
As suggested by the reviewer #2 in his point 4), here the "Stratigraphy" section was badly structured. Therefore we opted for adding a methodological section on the use of the UBSU criteria and adding to the "Stratigraphy" section a sub section on the "Facies analysis and eruptive style of volcanic centres".

Responding to the comments of reviewer 1#, in this sub section we made specific reference to the evolution of volcanic activity and eruptive style within older and younger eruptive units, highlighting that peak of explosive activity were reached only during the younger eruptive units.
Regarding Fig. 2, this figure was meant to illustrate a generic stratigraphy and elucidate the use of unconformity surfaces with different hierarchy to determine a relative chronology of the eruptive events, phase of syn- and inter- eruptive sedimentation and hence hiatuses in the volcanic activity. Correct references to the figure are now present in the text and a implemented caption now better explains the demonstrative value of this figure and the abbreviation (symbols) used therein. In particular we think that this figure has been interpreted by reviewer 1# to be a geological section thus creating confusion on the relation with the figure displaying the correlation between stratigraphic logs.

Regarding the comment of reviewer 1# on the correlation between stratigraphic sections, has been specified that the logs reported in Fig. 3 are the most representative among all the ones measured and reported in the geological map.
In particular it is important to note that stratigraphic sections are generally meant to complement information that are not immediately derivable from the map therefore the exact correspondence of map and logs is desirable but not always necessary. In particular the incongruences raised by reviewer #1 are determined by the small thickness of some deposits (generally below 1 meter thick) that crop out in the field and that cannot properly be represented in the map (at 1:10.000 scale as in our case) but have to be represented in the logs to account for the stratigraphic relationships between sedimentary bodies. This is a well-established convention in the production of geologic maps. Nevertheless we acknowledge reviewer 1# to have rightly pointed out this issue and other incongruences in the map and the stratigraphic logs, that have now been corrected.
Namely:

- the Upper Bosquet epiclastic unit on log 1 has been added
- the position of S2 unconformity in log 5 and 7 has been changed
- the Puig Martinyá and Puig Subiá (Santa Pau Syntem) eruptive centres have been added in the map and the stratigraphic summary of Fig. 4. Here lava flows have been associated to their respective eruptive centres.
- the Pre-volcanic sedimentary basement has been added in the stratigraphic summary of Fig. 4
- the position of the Fageda d'en Jordà lava in the stratigraphic summary of Fig. 4 (wrongly positioned in the early version) has been changed
- Position of main scoria cones named in the map of Fig. 4 are now reported in the other figures to facilitate orientation of the reader.

L257- 388 and Fig.7
As suggested by reviewer #2 in point 4), this section has been re-organized by including a methodological paragraph. In this section a new reference (Bonali et al., 2011) to the methodology has been added to the text. The text has been rearranged accordingly with specific reference to the modifications of Fig.7 suggested by reviewer #2. In particular in this figure we added a Fry plot to

support the analysis of the preferential orientation of volcanic vents. The plot has been introduced and explained in the text and in the figure caption.

L390 - 424 and Fig.8
Responding to the comments of reviewer 1#, here has been specified in the text that the isopachs maps reported in Fig. 8 represents the thickness of the volcanic deposits comprised between the pre-volcanic substrate and the topography with the exclusion of major scoria cones thickness. The elevation corresponding to major scoria cones has been removed from the isopachs map in order to better evidence the geometry of the sedimentary basin and its depocentres. In Fig. 8 the position of major scoria cones named in fig. 4 are now reported as reference.
We removed from Fig. 8 the wrong structural scheme and the inferred fault according to the comment raised by reviewer 2# in points 5 and 7.

L426 – 563
Also in the "Discussion" section we separated the information regarding the time evolution, the space evolution (as announced in the manuscript title) and the eruptive style and output rate of volcanism to discuss more clearly data and their interpretation.

L436
In response to the comment of reviewer 1# in the text, we specified here that the limited thickness of the paleosols were more likely determined by paleoclimatic conditions unfavorable to the formation of mature soils more than to erosion.

L451
The dating method has been specified as requested by reviewer 1# in the text.

L454 - 458
As suggested by reviewer 1# we also calculated the time gap between the Valls dels Arcs and Santa Pau synthems.

L467 – 488
We discussed more clearly the distribution of the cones and their morphological feature in light of the analysis of lineaments in the pre-volcanic basement and the stress tensor data as suggested by reviewer 2#, and removed the interpretation of the pull-apart basin. We also discussed more deeply the occurrence of cones along pre-existing lineaments adding the reference of a recent review paper on monogenetic cones alignment (Le Corvec et al., 2013). We also highlighted the occurrence of contemporaneous explosive activity (the youngest in the area) along a fracture oriented according to the present stress tensor (L 484 – 488) following the suggestions of both reviewers.

Sincerely

Corrado Cimarelli

Figure1
Click here to download high resolution image

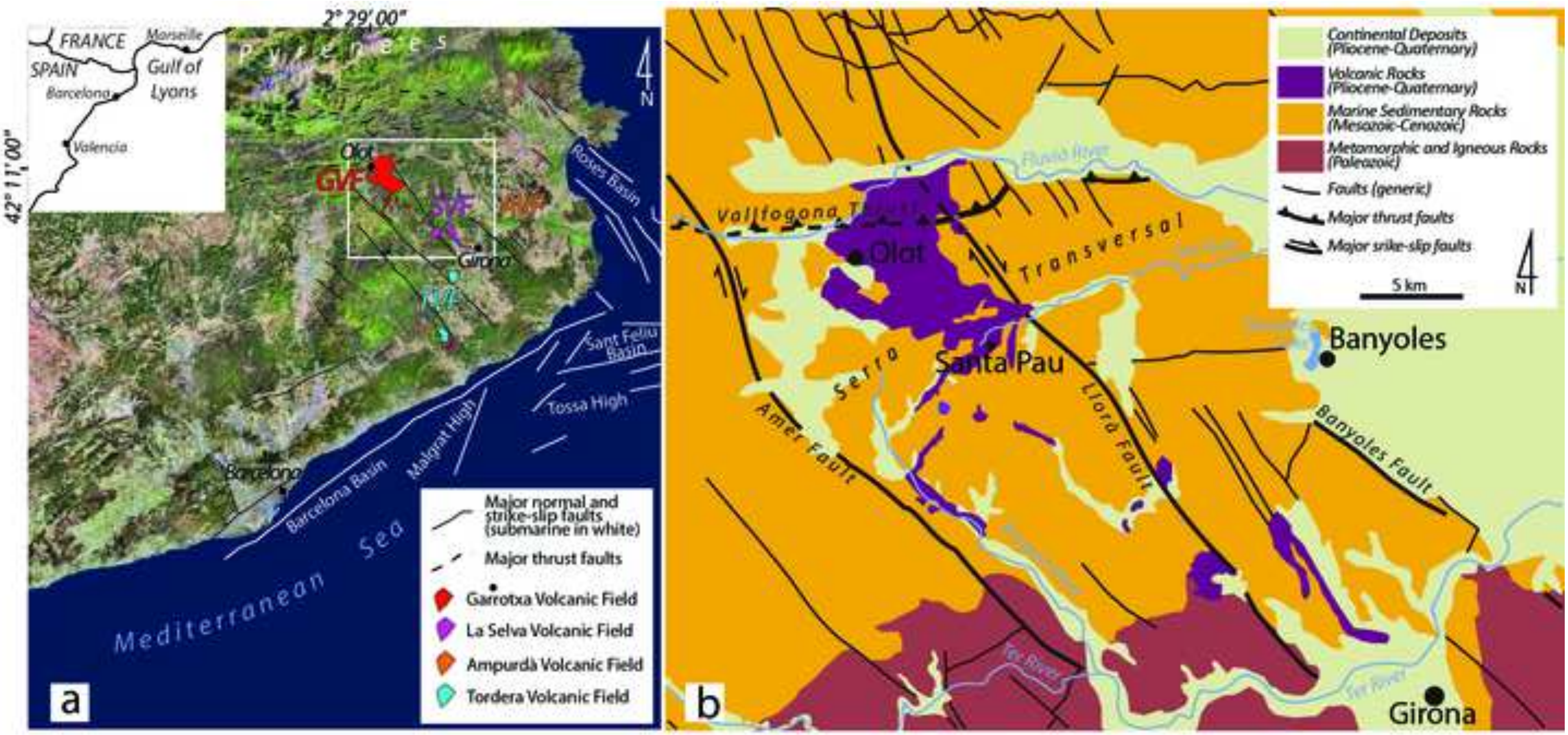

Figure2

Click here to download high resolution image

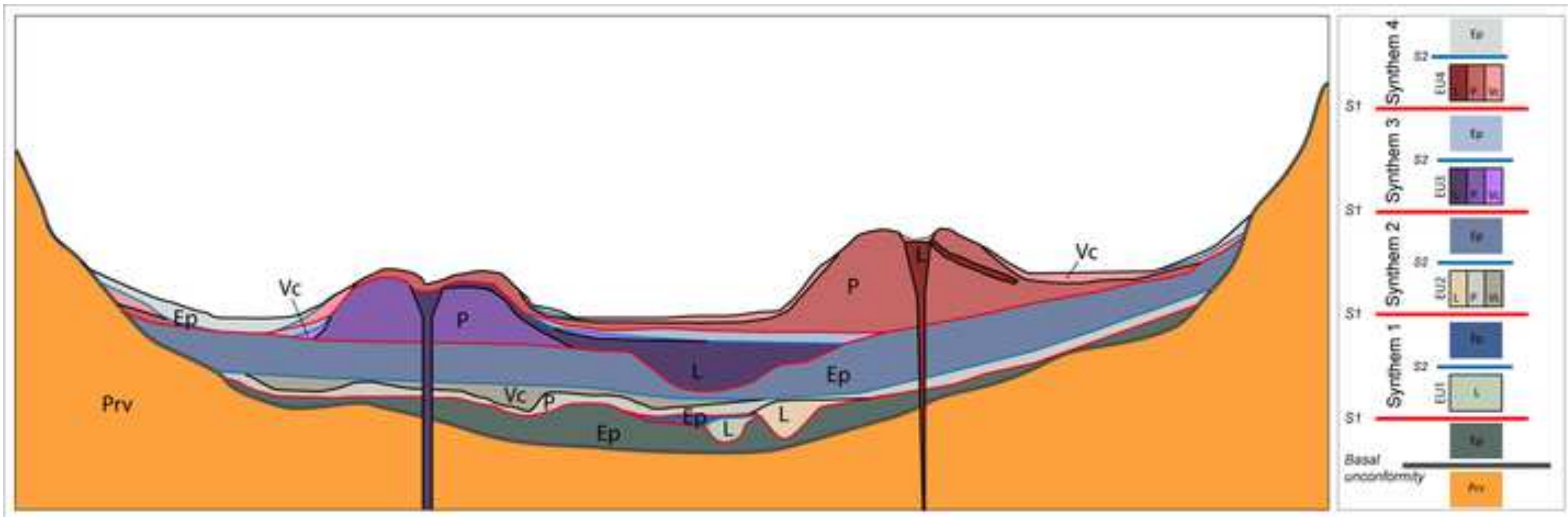

Figure3

Click here to download high resolution image

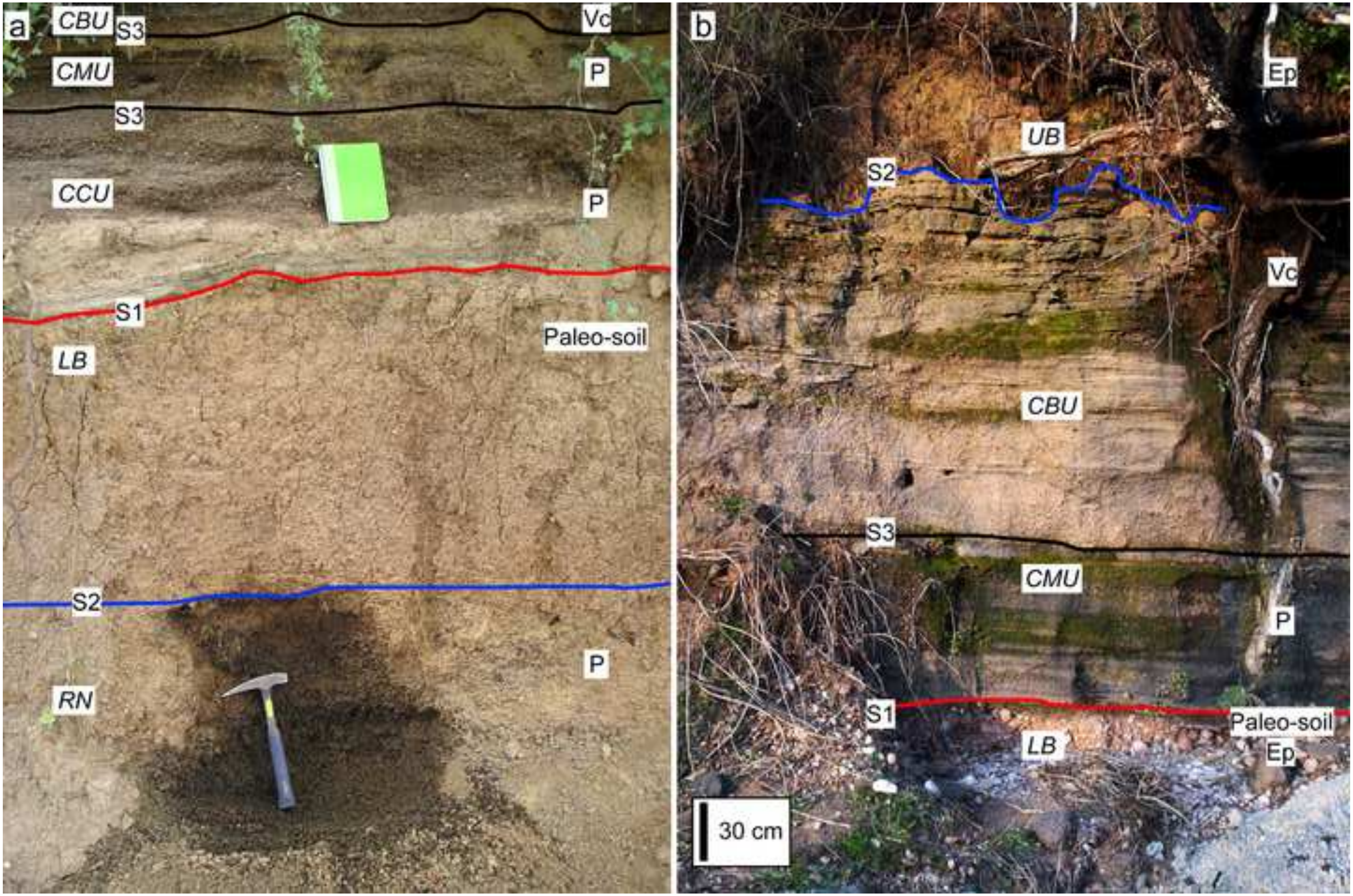

Figure4

Click here to download high resolution image

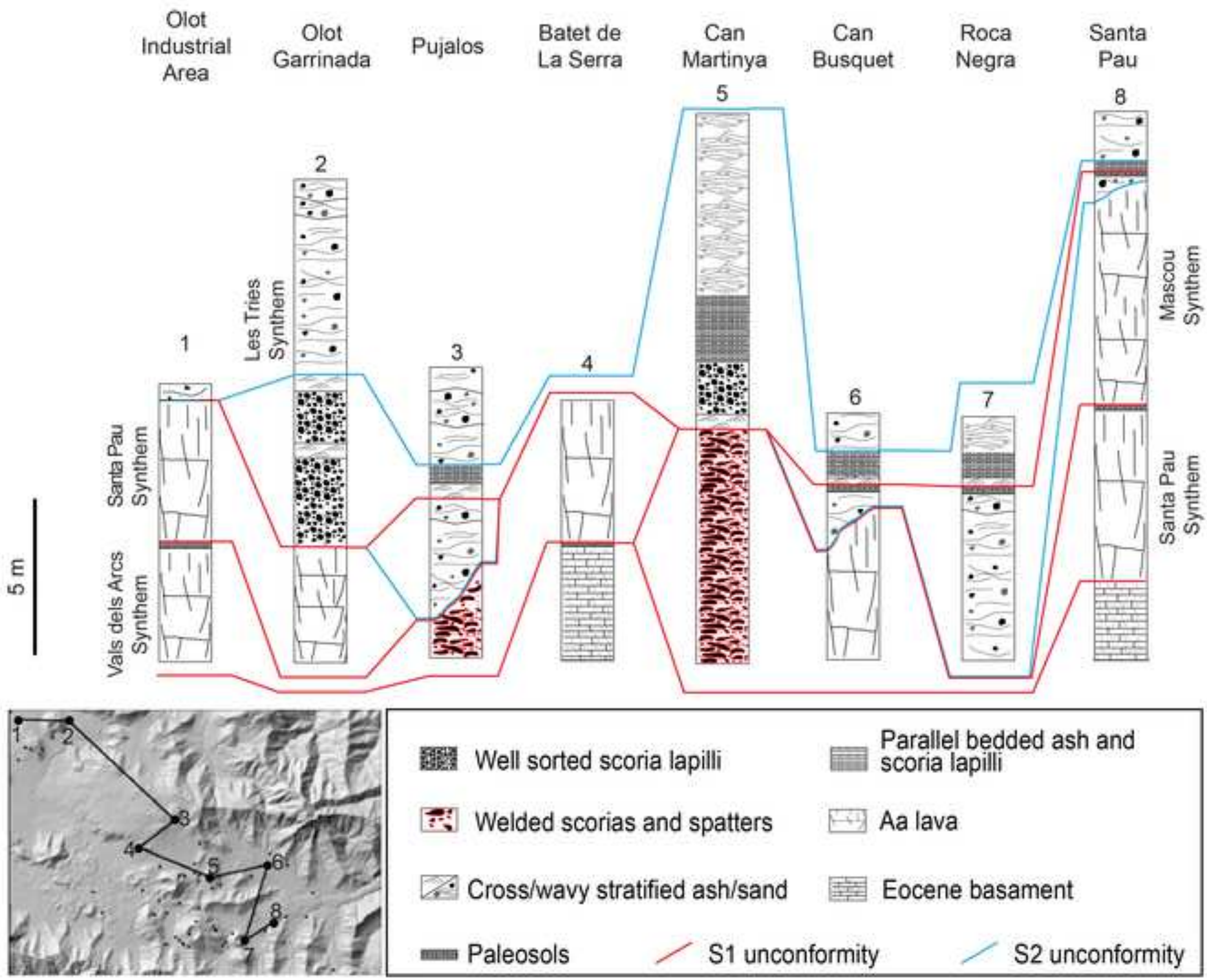

Figure5

Click here to download high resolution image

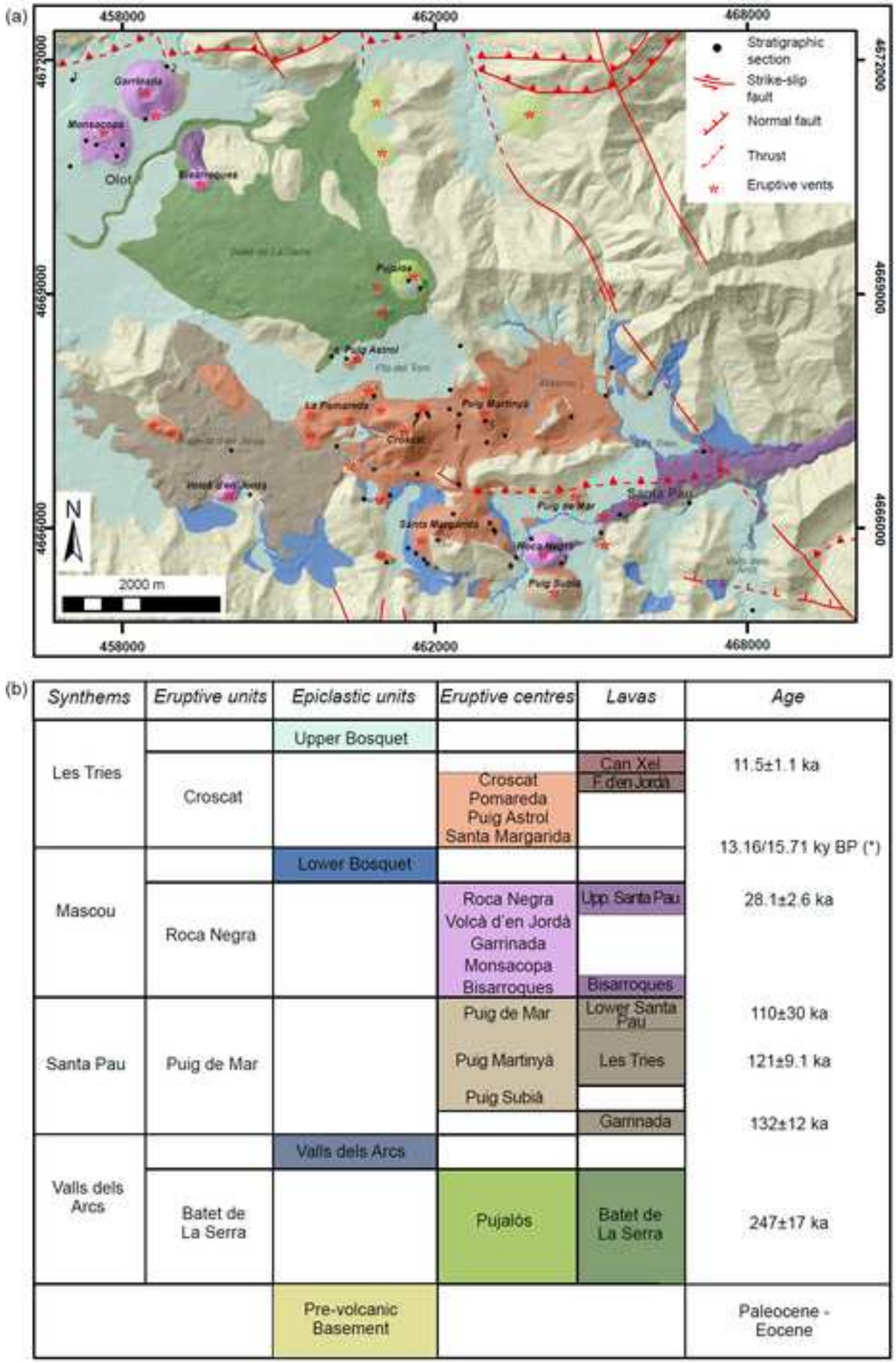

Figure6

Click here to download high resolution image

Figure7
Click here to download high resolution image

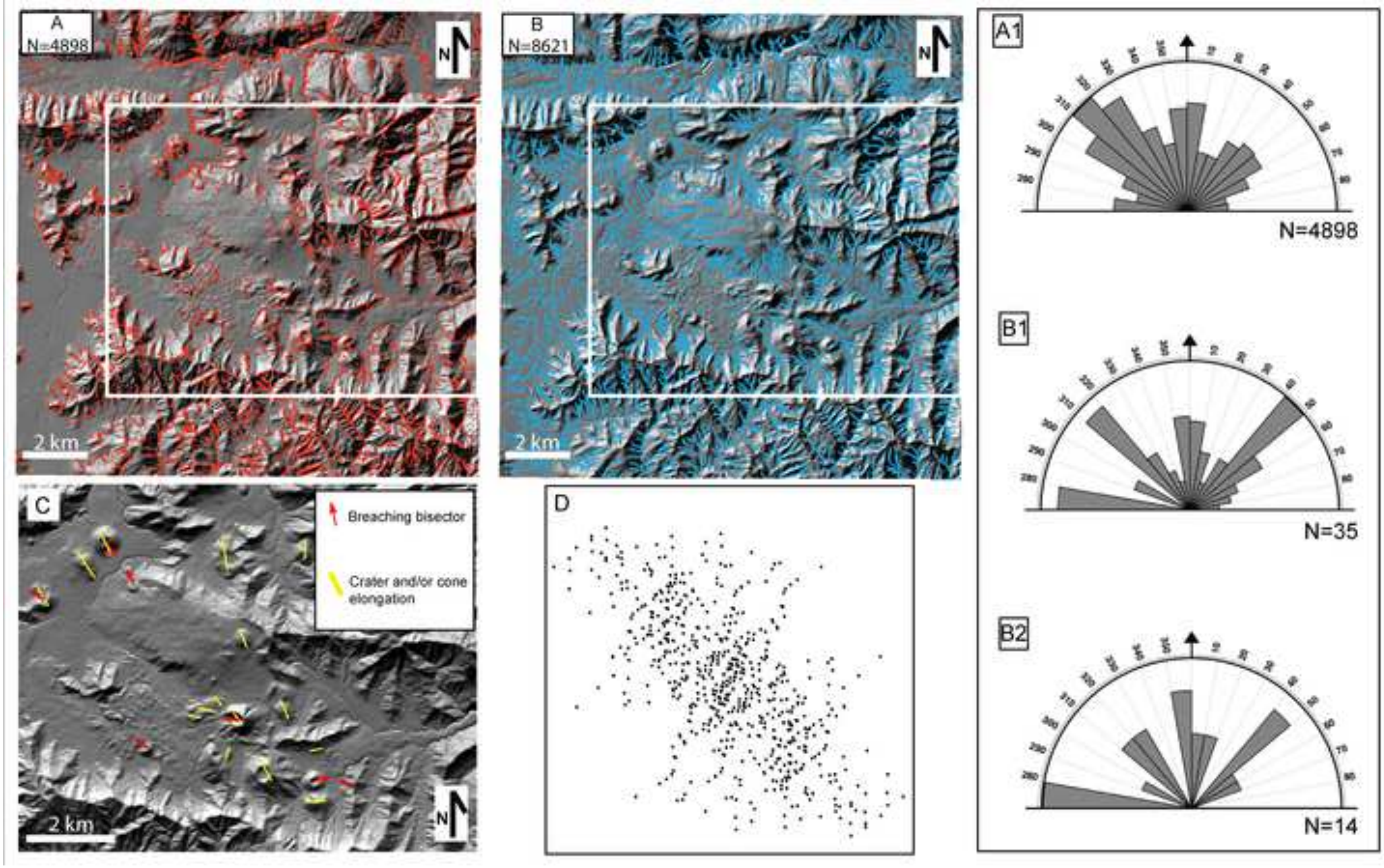

Figure8

Click here to download high resolution image

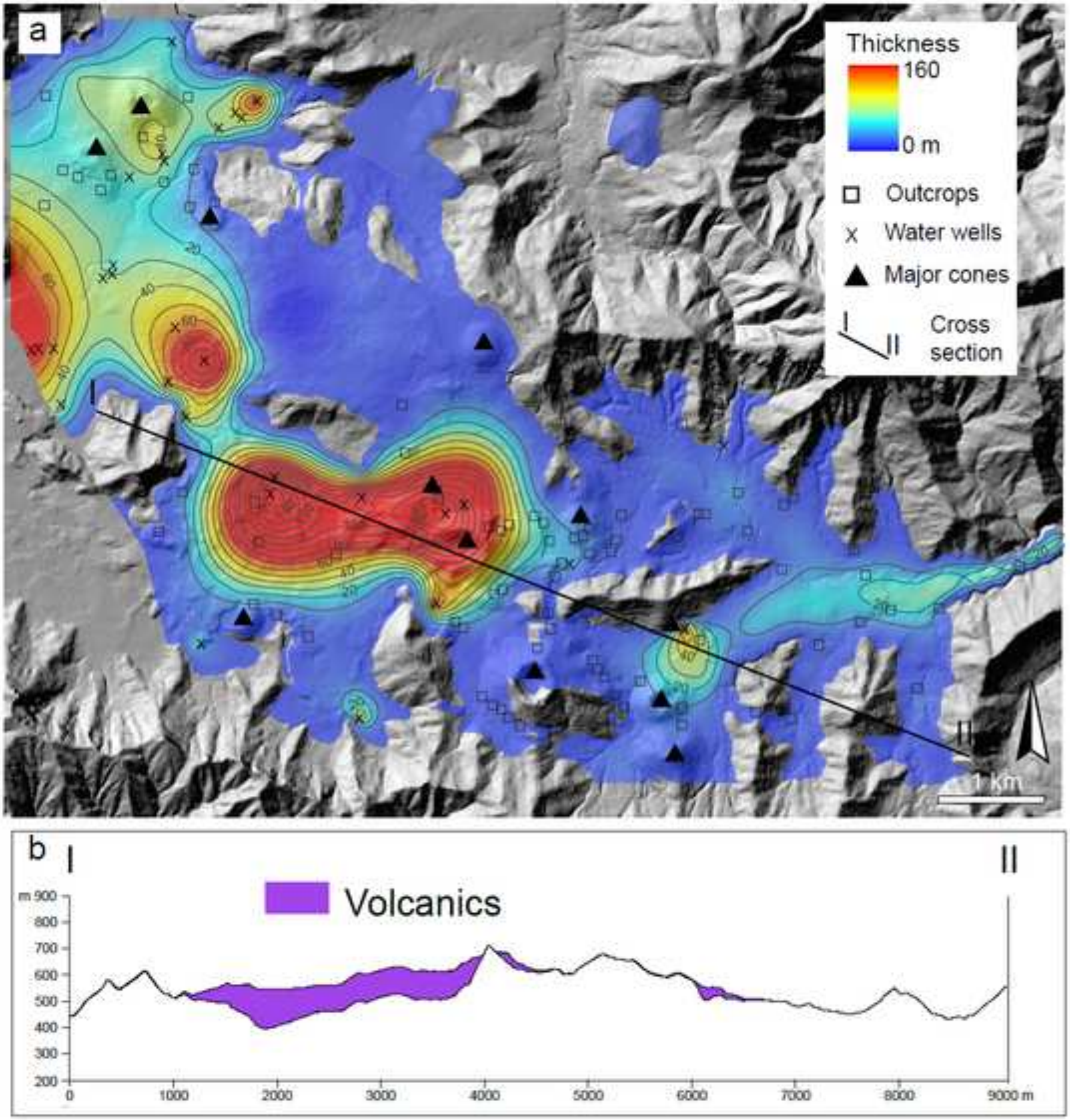

Figure9

Click here to download high resolution image

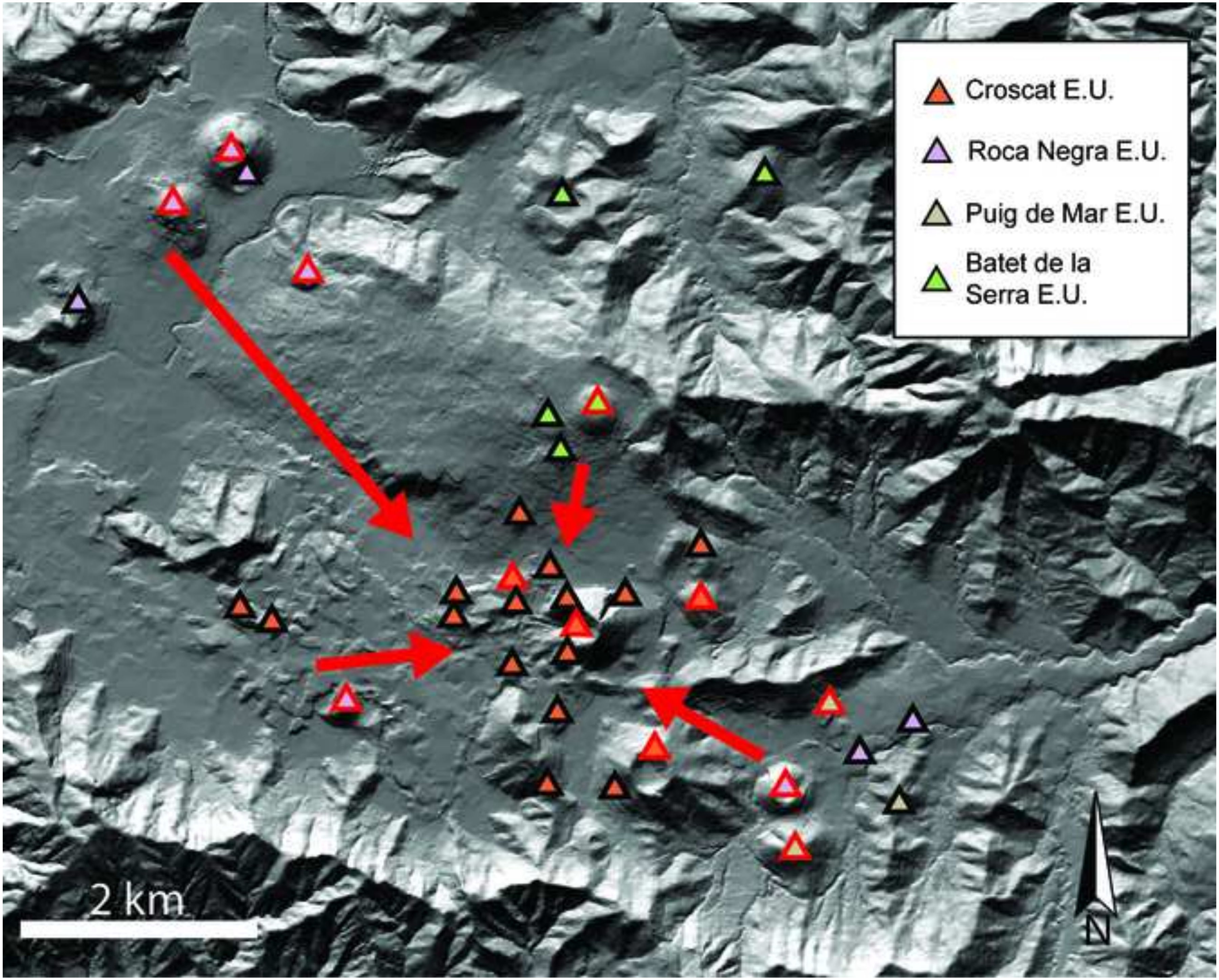

Figure10
Click here to download high resolution image

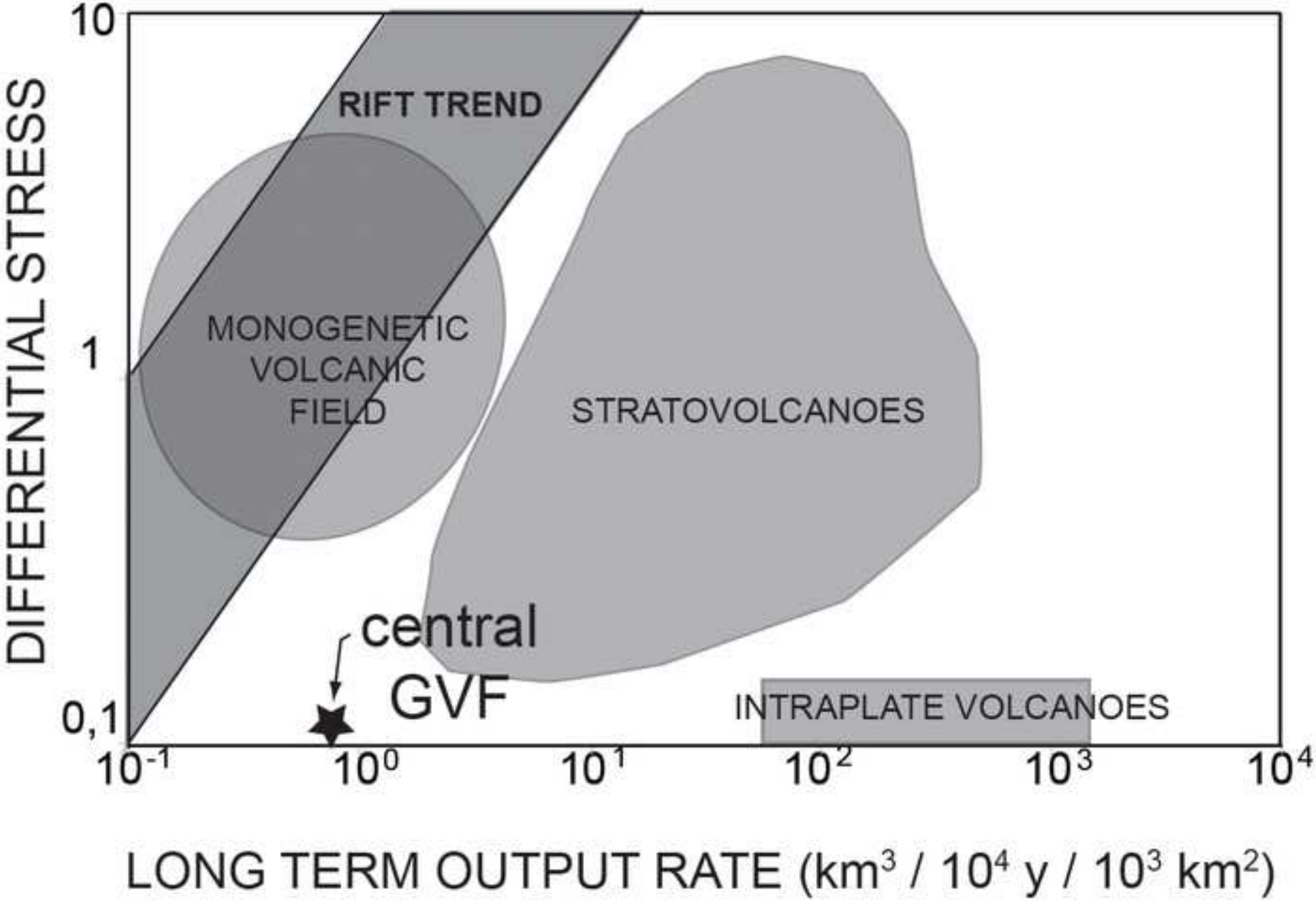

Table1

| Units | Description | Eruptive vents or source | Interpretation |
|---|---|---|---|
| Clot Sagalla Unit | *Bedding:* Absent<br>*Texture and Grading:*Massive, chaotic, matrix supported<br>*Clast size:* sandy matrix (40%); pebble clasts (60%)<br>*Clast type:*altered volcanic ashy-matrix; lava lithics and red spatter – type scoria.<br>*Clast Shape:* Sub – angular and platy shaped.<br>*Welding:* Absent<br>*Lithics/xenoliths:* Absent | | Deposits of the Croscat CSC western flank |
| Can Xel Lava | *Structure:* Massive to breciated<br>*Texture:* low porphiritic<br>*Phenocrysts:* ol, cpx and plg | Croscat CSC | Effusive activity |
| Can Barrca Unit | *Bedding:* Planar or low angle cross-bedded, 100 mm-thick beds (proximal phreatomagmatic); cross and planar-bedded, 10 to 50 mm-thick beds (medial and distal CMU reworked)<br>*Texture and Grading:* Each bed is normal graded in proximal preatomagmatic deposits) to reverse graded (medial and distal reworked CMU deposits)<br>*Clast size:* Fine to coarse ash (both in proximal and in distal deposits)<br>*Clast type:* Moderate to high vesicular scoriae<br>*Clast Shape:* Blocky to high-stretched clasts<br>*Welding:* Absent<br>*Lithics/xenoliths:* Lava lithics | Croscat CSC | Deposits of pulsatory phreatomagmatic explosions and syn- CMU reworked material |
| Can Martinyà Unit | *Bedding:* Planar, locally lenticular (proximal); planar (distal)<br>*Texture and Grading:* Reverse to normal graded (both in proximal and in distal deposits)<br>*Clast size:* Lapilli, with bomb lenses (proximal); Lapilli to coarse ash (distal)<br>*Clast type:* Moderate to high vesicular scoriae: dense bomb are also present<br>*Clast Shape:* Irregular to high-stretched clasts<br>*Welding:* Absent<br>*Lithics/xenoliths:* High-silica glass-bearing xenoliths (Buchites) | Croscat CSC | Fall-out deposits from violent Strombolian explosions |
| Upper Quesito Unit | *Bedding:* Mainly lenticular. Stratified, 20 mm-thick beds<br>*Texture and Grading:* Multiple reverse grading<br>*Clast size:* Lapilli, Bomb to lapilli<br>*Clast type:* Moderate vesicular scoriae<br>*Clast Shape:* Aerodinamic shape of bomb clasts, irregular shape of lapilli clasts<br>*Welding:* Local moderate welding<br>*Lithics/xenoliths:* Rare eocene calcarenitic xenoliths | Croscat CSC | Fall-out deposits from Strombolian explosions |

| | | | |
|---|---|---|---|
| Lower Quesito Unit | *Bedding: Mainly lenticular.* Crudely stratified<br>*Texture and Grading:* Massive to reverse grading<br>*Clast size:* Bomb, with minor lapilli<br>*Clast type:* Moderate vesicular scoriae and low vesicular spatter-type clasts<br>*Clast Shape:* Aereodinamic and fluidal shape, wrapping around underlying clasts<br>*Welding:* Partially welded over much of deposit exent<br>*Lithics/xenoliths:* Rare sanidine xenocrysts | Croscat CSC; Pomareda SpC; Santa Margarida SpC; Puig Astrol SpC; Undistinguished SpCs | Fall-out deposits from Hawaiian-fountaining explosions |
| Can Caselles Unit | *Bedding:* Planar, Cross-bedded, 10 to 100 mm-thick beds (proximal); cross-bedded to planar-bedded, 1 to 10 mm-thick beds (distal)<br>*Texture and Grading:* Each bed is normal graded (both in proximal and in distal deposits)<br>*Clast size:* Lapilli, Fine to coarse ash (proximal); Fine ash (distal)<br>*Clast type:* Moderate to high vesicular scoriae<br>*Clast Shape:* Blocky to high-stretched clasts<br>*Welding:* Absent<br>*Lithics/xenoliths:* Aboundant sandstones, marls and clacarenitics; lava lithics are also present | Santa Margarida SpC | Dilute pyroclastc density current deposits from intermittent phreatomagmatic explosions |
| Upper Santa Pau Lava | *Structure:* massive to columnar jointed, sometimes pseudo-hyaloclastc. The base is brecciated<br>*Texture:* low porphiritic<br>*Phenocrysts:* ol, cpx and plg<br>*Lithics/xenoliths:* gabbroid, pyroxenitic and amphibolitic | Roca Negra SC | Effusive activity |
| Roca Negra Unit | *Bedding:* Mainly lenticular; stratified, 200-500 mm-thick beds<br>*Texture and Grading:* Multiple reverse grading<br>*Clast size:* Lapilli, Bomb to lapilli<br>*Clast type:* Moderate to dense vesicular scoriae<br>*Clast Shape:* Aerodinamic shape of bomb clasts, irregular shape of lapilli clasts<br>*Welding:* Absent<br>*Lithics/xenoliths:* gabbroid, pyroxenitic and amphibolitic | Roca Negra SC | Fall-out deposits from Strombolian explosions |
| Volcà d'en Jordà | *Bedding:* Mainly lenticular; stratified, 200-300 mm-thick beds<br>*Texture and Grading:* Multiple reverse grading<br>*Clast size:* Lapilli, Bomb to lapilli<br>*Clast type:* Moderate vesicular scoriae<br>*Clast Shape:* Aerodinamic shape of bomb clasts, irregular shape of lapilli clasts<br>*Welding:* Local moderate welding<br>*Lithics/xenoliths:* Absent | Volcà d'en Jordà SC | Fall-out deposits from Strombolian explosions |

| | | | |
|---|---|---|---|
| La Cambrafosca | *Bedding:* Mainly lenticular; stratified, 100-200 mm-thick beds<br>*Texture and Grading:* Multiple reverse grading<br>*Clast size:* Lapilli, Bomb to lapilli<br>*Clast type:* Moderate vesicular scoriae<br>*Clast Shape:* Aerodinamic shape of bomb clasts, irregular shape of lapilli clasts<br>*Welding:* Local moderate welding<br>*Lithics/xenoliths:* Eocene sedimentary blocks | La Cambrafosca eruptive vents | Fall-out deposits from Strombolian explosions |
| Upper Garrinada | *Bedding:* Mainly lenticular; massive to broadly stratified, 100-200 mm-thick beds<br>*Texture and Grading:* Massive, mainly chaotic<br>*Clast size:* ashy matrix (60% - 20%); lapilli clasts<br>*Clast type:* Low vesicular scoriae<br>*Clast Shape:* angular clasts<br>*Welding:* no welding, cohesive<br>*Lithics/xenoliths:* crystal-rich ash matrix; very abundant cm-sized black lava, grey altered lava and calcarenitic clasts | La Garrinada CSC | Pyroclastic density current and fall-out deposit from phreatomagmatic/phreatic explosions |
| Lower Garrinada | *Bedding:* Mainly lenticular; stratified, 300-500 mm-thick beds (LGU1); planar to cross-bedded, 10-100 mm-thick beds (LGU2)<br>*Texture and Grading:* Multiple reverse grading (LGU1); alternate (LGU2)<br>*Clast size:* Bomb to lapilli (LGU1); lapilli and ash (LGU2)<br>*Clast type:* Moderate to vesicular scoriae (both LGU1 and LGU2)<br>*Clast Shape:* Irregular shape clasts (LGU1); irregular to blocky shaped particles, with frequent palagonizzation (LGU2)<br>*Welding:* Absent<br>*Lithics/xenoliths:* Lava lithics | La Garrinada CSC | Fall-out deposits from Strombolian explosions (LGU1); fall-out and dilute pyroclastic density current from phreatomagmatic expllosions |
| Upper Monsacopa | *Bedding:* Cross-bedded, 50 to 200 mm-thick beds (proximal); Cross-bedded to planar-bedded, 10 to 50 mm-thick beds (distal)<br>*Texture and Grading:* Each bed is normal graded (both in proximal and in distal deposits)<br>*Clast size:* Lapilli to coarse ash (proximal); fine to coarse ash (distal)<br>*Clast type:* Moderate to high vesicular scoriae<br>*Clast Shape:* Blocky to high-stretched clasts<br>*Welding:* Absent<br>*Lithics/xenoliths:* Lava lithics | Monsacopa CSC | |
| Lower Monsacopa | *Bedding:* Mainly lenticular; stratified, 200-500 mm-thick beds<br>*Texture and Grading:* Multiple reverse grading<br>*Clast size:* Lapilli, Bomb to lapilli<br>*Clast type:* Moderate to dense vesicular scoriae<br>*Clast Shape:* Aerodinamic shape of bomb clasts, irregular shape of lapilli clasts<br>*Welding:* Absent | Monsacopa CSC | Fall-out deposits from Strombolian explosions |

| | | | |
|---|---|---|---|
| | *Lithics/xenoliths:* gabbroid, pyroxenitic and amphibolitic | | |
| Bisarroques Lava | *Structure:* clastogenic<br>*Texture:* low porphiritic<br>*Phenocrysts:*ol, cpx and plg<br>*Lithics/xenoliths:* Absent | Bisarroques SpC | agglutination and flow of hot juvenile fragments from Hawaiian fountaining |
| Bisarroques Unit | *Bedding: Mainly lenticular.* Crudely stratified<br>*Texture and Grading:* Massive to reverse grading<br>*Clast size:* Bomb, with minor lapilli<br>*Clast type:* Moderate vesicular scoriae and low vesicular spatter-type clasts<br>*Clast Shape:* Aereodinamic and fluidal shape, wrapping around underlying clasts<br>*Welding:* Partially welded over much of deposit exent<br>*Lithics/xenoliths:* Absent | Bisarroques SpC | Fall-out deposits from Hawaiian-fountaining explosions |

| | | | |
|---|---|---|---|
| Fageda d'en Jordà Phase | *Structure:* lava mounds, massive to jointed, with columnar and radial jointing<br>*Texture:* low porphiritic<br>*Phenocrysts:*ol, cpx and plg<br>*Lithics/xenoliths:* Absent | Eruptive fissures in the Fageta d'en Jordà area | Large effusive activity |
| Lower Santa Pau Lava | *Structure:* massive to columnar jointed; the base is brecciated<br>*Texture:* low porphiritic<br>*Phenocrysts:*ol, cpx and plg<br>*Lithics/xenoliths:* Absent | Eruptive fissures between Puig the Mar SpC and Volcà d'en Simò SpC | Effusive activity |
| Les Tries Lava | *Structure:* massive to columnar jointed; the base is brecciated<br>*Texture:* low porphiritic<br>*Phenocrysts:*ol, cpx and plg<br>*Lithics/xenoliths:* Absent | Eruptive fissures near Puig de Martinyà area | Effusive activity |
| Garrinada Lava | *Structure:* massive to columnar jointed; the base is brecciated<br>*Texture:* low porphiritic<br>*Phenocrysts:*ol, cpx and plg<br>*Lithics/xenoliths:* Absent | Eruptive fissure in the Monsacopa – Garrinada area | Effusive activity |
| Les Cases Noves Unit | *Bedding:* Mainly lenticular<br>*Texture and Grading:* Massive, mainly chaotic<br>*Clast size:* ashy matrix (90% - 60%); lapilli clasts<br>*Clast type:* Moderate vesicular scoriae<br>*Clast Shape:* angular to irregular clasts<br>*Welding:* Absent, cohesive<br>*Lithics/xenoliths:* cm-sized black lava, grey altered lava, calcarenitic and marl clasts | Source in the Puig de Mar – Volcà d'en Simò area | Syn-eruptive reworked deposits |

| | | | |
|---|---|---|---|
| Puig de Mar Phase | *Bedding: Mainly lenticular.* Crudely stratified<br>*Texture and Grading:* Massive to reverse grading<br>*Clast size:* Bomb, with minor lapilli<br>*Clast type:* Moderate vesicular scoriae and low vesicular spatter-type clasts<br>*Clast Shape:* Aereodinamic and fluidal shape, wrapping around underlying clasts<br>*Welding:* Partially welded over much of deposit extent<br>*Lithics/xenoliths:* Rare sanidine xenocrysts | Puig de Mar SpC; Puig de Martinyà SpC; Volcà d'en Simò SpC; Puig Subià SpC; Undistinguished SpCs | Fall-out deposits from Hawaiian-fountaining explosions |

| | | | |
|---|---|---|---|
| Pujalos Phase | *Bedding: Mainly lenticular.* Crudely stratified<br>*Texture and Grading:* Massive to reverse grading<br>*Clast size:* Bomb, with minor lapilli<br>*Clast type:* Moderate vesicular scoriae and low vesicular spatter-type clasts<br>*Clast Shape:* Aereodinamic and fluidal shape, wrapping around underlying clasts<br>*Welding:* Partially welded over much of deposit exent<br>*Lithics/xenoliths:* Absent | Pujalos SpC; Undistinguished SpCs | Fall-out deposits from Hawaiian-fountaining explosions |
| Batet de La Serra Lava | *Structure:* massive to columnar jointed; the base is brecciated<br>*Texture:* low porphiritic<br>*Phenocrysts:*ol, cpx and plg<br>*Lithics/xenoliths:* Absent | Eruptive fissures in the Batet de La Serra high-plain, near Pujalos SpC | Large effusive activity |

Table2

| **Type of reworked deposit** | **Facies description** |
|---|---|
| Syn-eruptive | *Bedding:* Lenticular<br>*Texture and Grading:*Massive, chaotic to reverse graded, clast-supported<br>*Clast size:* ash to bombs and blocks<br>*Clast type:*fresh to altered juvenile clasts (monomictic); lava lithics; crystals<br>*Clast Shape:* Sub – angular. |
| Early post-eruptive | *Bedding:* Lenticular to low angle cross-bedded (proximal to the source), planar to low-angle cross bedded (medial to distal from the source)<br>*Texture and Grading:*Massive to reverse graded, clast- to matrix-supported<br>*Clast size:* ash to lapilli<br>*Clast type:* altered to fresh juvenile clasts (monomictic); lava lithics; crystals<br>*Clast Shape:* Sub – angular. |
| Late post-eruptive | *Bedding:* Lenticular to low angle cross-bedded (proximal to the source), planar to low-angle cross bedded (medial to distal from the source)<br>*Texture and Grading:*Massive to reverse graded, clast- to matrix-supported<br>*Clast size:* sand and pebbles<br>*Clast type:* altered juvenile clasts (polimictic); lava lithics; Eocene sedimentary clasts (rare or concentrated in lenses)<br>*Clast Shape:* Sub – angular to sub-rounded. |
| Inter-eruptive | *Bedding:* Not bedded, lenticular to low angle cross-bedded<br>*Texture and Grading:*Massive, chaotic or reverse to normal graded, clast- to matrix-supported<br>*Clast size:* sand and pebbles (near the source), sand and silt (plain facies)<br>*Clast type:* Eocene sedimentary clasts, altered juvenile clasts (polimictic); lava lithics<br>*Clast Shape: S*ub-rounded to sub – angular. |

Table3

| *Cone Name* | **Croscat** | **Garrinada** | **Monsacopa** | **Puig Subià** | **Roca Negra** | **Puig Jordà** | **Pomareda** |
|---|---|---|---|---|---|---|---|
| ***Cone Volume (x $10^6$ $m^3$) DRE*** | 10,22 | 12 | 7,11 | 8,44 | 4,89 | 0,89 | 10,67 |
| ***Tephra Blancket Volume (x $10^6$ $m^3$) DRE*** | 13,66 | none | 0,8 | none | none | none | none |
| ***Related Lava Flow Volume (x $10^6$ $m^3$)*** | 10 | none | none | none | 5,2 | none | 0 |
| ***Total Volume (x $10^6$ $m^3$) DRE*** | 33,88 | 12 | 7,91 | 8,44 | 10,09 | 0,89 | 10,67 |
| ***Cone Basal Area ($km^2$)*** | 0,74 | 0,53 | 0,35 | 0,3 | 0,2 | 0,6 | 0,55 |
| ***Tephra Dispersal Area ($km^2$)*** | 8 | 0,53 | 0,41 | none | none | none | none |
| ***Related Lava Flow Area ($km^2$)*** | 0,05 | none | none | none | 1,04 | none | 0 |
| ***Cone Hight (m)*** | 189,04 | 128,03 | 97,17 | 144,35 | 110,2 | 63,42 | 31,38 |
| ***Outer Slope Angle*** | 25 | 26 | 23 | 23 | 28 | 25 | 20 |
| ***Basament dip angle*** | 0 | 0 | 0 | <10 | <10 | <10 | 0 |
| ***Max elong. Axis lenght (m)*** | | 798 | 778 | 670 | | | 1255 |
| ***Max elong. Axis azimuth*** | | N154 | N135 | N088 | | | N057 |
| ***Crater rim depressed point allignament*** | | N334 | N315 | | | | |
| ***Breaching direction*** | N267 | | | | N055 | N295 | |

| ***Cone Name*** | **Pujalos** | **Santa Margarida** | **Puig Astrol** | **Puig de Mar** | **Bisarroques** | **Sant Miquel Sacot** | **Puig Simò** |
|---|---|---|---|---|---|---|---|
| ***Cone Volume (x 106 $m^3$) DRE*** | 1,78 | 1,78 | 0,04 | 1,69 | 0,27 | 0,22 | 0,18 |
| ***Tephra Blancket Volume (x $10^6$ $m^3$) DRE*** | none | none | none | none | none | none | none |
| ***Related Lava Flow Volume (x $10^6$ $m^3$)*** | 13,34 | none | none | 5,85 | 0,24 | none | none |
| ***Total Volume (x $10^6$ $m^3$) DRE*** | 15,12 | 1,78 | 0,04 | 7,54 | 0,51 | 0,22 | 0,18 |
| ***Cone Basal Area ($km^2$)*** | 0,13 | 0,11 | 0,01 | 0,12 | 0,04 | 0,02 | 0,02 |
| ***Tephra Dispersal Area ($km^2$)*** | none | none | none | none | none | none | none |
| ***Related Lava Flow Area ($km^2$)*** | 6,67 | none | none | 1,17 | 0,12 | | none |
| ***Cone Hight (m)*** | 59,51 | 80,78 | 30,93 | 77,41 | 49,33 | 48,55 | 39,77 |
| ***Outer Slope Angle*** | 18 | 24 | 20 | 25 | 19 | 20 | 15 |
| ***Basament dip angle*** | <10 | >10 | 10 | <10 | >10 | >10 | >10 |
| ***Max elong. Axis lenght (m)*** | 516 | | | 581 | | | |
| ***Max elong. Axis azimuth*** | N167 | | | 73 | | | |
| ***Crater rim depressed point allignament*** | N000 | | | | | | |
| ***Breaching direction*** | | | | | N347 | | N124 |